

## DHA dietary intervention caused different hippocampal lipid and protein profile in ApoE<sup>-/-</sup> and C57BL/6J mice

Lu Liu<sup>a,b,1</sup>, Jingjing Xu<sup>a,b,1</sup>, Xiaochen Huang<sup>a</sup>, Ying Wang<sup>c</sup>, Xiaojun Ma<sup>a,b</sup>, Xixiang Wang<sup>a,b</sup>, Yu Liu<sup>a,b</sup>, Xiuwen Ren<sup>a,b</sup>, Jiahao Li<sup>a,b</sup>, Yueyong Wang<sup>a,b</sup>, Shaobo Zhou<sup>d,\*</sup>, Linhong Yuan<sup>a,b,\*\*</sup>

<sup>a</sup> School of Public Health, Capital Medical University, Beijing, China

<sup>b</sup> China-British Joint Laboratory of Nutrition Prevention and Control of Chronic Diseases

<sup>c</sup> Suzhou Hospital, Affiliated Hospital of Medical School, Nanjing University, Suzhou, China

<sup>d</sup> School of Science, Faculty of Engineering and Science, University of Greenwich, Central Avenue, Chatham ME4 4TB, UK

### ARTICLE INFO

#### Keywords:

ApoE<sup>-/-</sup> mice

DHA

Dietary intervention, proteomics

Lipidomics

### ABSTRACT

**Background:** Changes in protein and lipid levels may occur in the Alzheimer's disease brain, and DHA can have beneficial effects on it. To investigate the impact of DHA dietary intervention on brain protein and lipid profile in ApoE<sup>-/-</sup> mice and C57 mice.

**Method:** Three-month-old ApoE<sup>-/-</sup> mice and C57 mice were randomly divided into two groups respectively, and fed with control diet and DHA-fortified diet for five months. Cortical TC, HDL-C and LDL-C levels and cholesterol metabolism-related protein expression were measured by ELISA or immunohistochemistry methods. Hippocampus were collected for proteomic and lipidomics analysis by LC-MS/MS and differential proteins and lipid metabolites were screened and further analyzed by GO functional annotation and KEGG pathway enrichment analysis.

**Results:** DHA intervention decreased cortical TC level in both C57 and ApoE<sup>-/-</sup> mice ( $P < 0.05$ ), but caused different change of cortical HDL-C, LDL-C level and LDL-C/HDL-C ratio in C57 and ApoE<sup>-/-</sup> mice ( $P < 0.05$ ). Discrepant cortical and hippocampal LDLR, ABCG1, Lox1 and SORT1 protein expression was found between C57 and ApoE<sup>-/-</sup> mice ( $P < 0.05$ ), and DHA treatment caused different changes of these proteins in C57 and ApoE<sup>-/-</sup> mice ( $P < 0.05$ ). Differential hippocampal proteins and lipids profile were found in C57 and ApoE<sup>-/-</sup> mice before and after DHA treatment, which were mainly involved in vesicular transport and phospholipid metabolic pathways.

**Conclusion:** ApoE genetic defect caused abnormal cholesterol metabolism, and affected protein and lipid profile, as well as discrepant response of hippocampal protein and lipids profile in the brain of mice given DHA fortified diet intervention.

### 1. Introduction

Alzheimer's disease (AD) is a degenerative disease of the central nervous system, and there are a great number of existing patients with AD in China. Due to the increasing aging population in China, the number of aging subjects with AD increased dramatically, and the number of AD patients in China was estimated to account for 1/4 of the total number of cases worldwide by 2030 [1]. The pathology of AD mainly includes the formation of neurofibrillary tangles and senile

plaques in the brain, and these changes are evident in specific brain regions, and the hippocampus is one of the first cerebral areas to be affected [2].

As one of the proteins mainly involving in the metabolism and transport of lipids *in vivo*, Apolipoprotein E (ApoE) is highly expressed in the brain [3]. There is growing evidence indicating that ApoE plays a key role in the integrity, function, and repair of the central nervous system after neuron injury [4]. The defect of ApoE gene induced distribution of lipid metabolism has been reported by previous studies [5,

\* Corresponding author.

\*\* Corresponding author at: School of Public Health, Capital Medical University, Beijing, China.

E-mail addresses: [s.zhou@greenwich.ac.uk](mailto:s.zhou@greenwich.ac.uk) (S. Zhou), [yihmedu@126.com](mailto:yihmedu@126.com) (L. Yuan).

<sup>1</sup> These authors contribute equally to the work.

<https://doi.org/10.1016/j.bioph.2024.117088>

Received 26 May 2024; Received in revised form 28 June 2024; Accepted 1 July 2024

Available online 6 July 2024

0753-3322/© 2024 The Authors. Published by Elsevier Masson SAS. This is an open access article under the CC BY-NC license (<http://creativecommons.org/licenses/by-nc/4.0/>).

6]. Compared to C57BL/6 J (C57) mice, ApoE-deficient (ApoE<sup>-/-</sup>) mice showed higher level of plasma lipids and greater hepatic lipid deposition, such as total cholesterol (TC) and low-density lipoprotein cholesterol (LDL-C), and are more prone to develop hyperlipidemia [7]. Therefore, ApoE<sup>-/-</sup> mice have been widely used as a model for studying the relation between lipid metabolism abnormality and AD.

Abnormal lipid metabolism commonly observed in the brain of AD patient. Population-based study indicated that increased serum concentration of TC, LDL-C, non-high-density lipoprotein cholesterol (non-HDL-C), and LDL-C/HDL-C ratio positively correlated with the acceleration of global cognitive decline [8]. Disorder of cholesterol homeostasis in the brain is thought to be a key factor in the pathogenesis of AD [9], as cholesterol is transported primarily to the brain after binding to ApoE, participating in the formation of plasma membrane and axon myelin sheath, and facilitating the transmission of electroneurographic signals [10].

Docosahexaenoic acid (DHA) is an n-3 polyunsaturated fatty acid (PUFA). Various health benefits of DHA have been reported, such as enhancing cognitive function, promoting neuroplasticity, and improving neuropathy [11]. The regulatory effects of DHA on lipid metabolism were demonstrated by published documents. For example, DHA is effective in reducing circulating cholesterol and triglycerides levels, and increasing HDL-C concentration, enabling the body to maintain normal lipid metabolism homeostasis [12].

To date, few studies have reported the impacts of DHA dietary intervention on cerebral protein and lipid profile under different ApoE status. In this study, proteomics and lipidomics analysis were applied to investigate the effects of DHA dietary intervention on brain protein and lipid profile in ApoE<sup>-/-</sup> and C57 mice, aiming to clarify the potential molecular and related signaling pathways involving in the regulatory impacts of DHA dietary intervention on brain protein and lipid profile, and to reveal the potential mechanisms.

## 2. Materials and methods

### 2.1. Animals and treatments

Three-month-old C57 mice and ApoE<sup>-/-</sup> mice were purchased from the experimental animal center of Capital Medical University. According to the baseline body weight, C57 and ApoE<sup>-/-</sup> mice were randomly split into the control (feeding with normal diet) group and DHA-fortified diet group, respectively. There were 12 mice in each group (half male and half female). The animals were allowed to access to food and water freely. Mice were housed at room temperature with a 12-hour light-dark cycle. The animal experiment protocols were performed according to the guide for the care and use of laboratory animals (AEEI-2015-040). Mice in control group were given a normal control diet, and the mice in the intervention group were treated with a DHA-fortified diet for 5 months.

**Table 1**

Nutrient composition of control and intervention diets (g/kg).

	Control diet	DHA intervention diet
<b>Ingredients</b>		
Casein	70	70
Potato starch	215	215
Sucrose	50	50
Cellulose	25	25
L-cysteine	1.5	1.5
Choline hydrogen	0.9	0.9
Corn oil	27	22
Lard	13	13
Fish oil powder	0	5
Maltodextrin	125	125
<b>kcal%</b>		
Protein	14.7	14.7
Carbohydrates	75.9	75.9
Fat	9.4	9.4

The composition of experimental diet is listed in Table 1. Fish oil powder was purchased from DSM Nutritional Products Ltd. (Switzerland). According to previous studies, a diet containing DHA (3.6–13 g/kg) resulted in alterations of lipids and DHA levels in the brain [13,14]. Therefore, diet containing DHA of 5.5 g/kg was applied for dietary intervention in present study. The dietary intake and body weight of mice were recorded weekly during the experiment period.

### 2.2. Biological sample collection

At the end of dietary intervention, the mice were slaughtered and the cortical and hippocampal tissues were collected, and then stored immediately at  $-80^{\circ}\text{C}$  for biochemical, histological, and proteomic measurement.

### 2.3. Measurement of cortical cholesterol

Cortical TC, HDL-C, and LDL-C levels were measured using the assay kits from Nanjing Jiancheng (Nanjing, China) according to the manufacturer's instructions. Briefly, cortical tissues were weighed accurately, and 0.9 % sodium chloride solution was added [weight (g): volume (mL), 1:9], then homogenized mechanically in an ice water bath and centrifuged at 2500 rpm for 10 min. After that, the supernatant was collected for the measurements.

### 2.4. Immunohistochemistry

Immunohistochemistry (IHC) assays were performed according to the manufacturer's instructions. Briefly, deparaffinized and hydrated tissues were placed in 3 %  $\text{H}_2\text{O}_2$  and incubated at room temperature in darkness for 25 min. After washing with PBS (pH 7.4), the samples were then incubated in 3 % BSA for 30 min to reduce non-specific binding. After incubating primary antibody overnight at  $4^{\circ}\text{C}$  with anti-low-density lipoprotein receptor (LDLR) (1:1000, Abcam, UK), anti-adenosine triphosphate-binding cassette transporter G1 (ABCG1) (1:1000, Abcam, UK), anti-sortilin 1 (SORT1) (1:1000, Abcam, UK) and anti-lectin-like oxidized low-density lipoprotein receptor-1 (LOX1) (1:1000, Abcam, UK) respectively.

The tissues were then washed in PBS and incubated with secondary antibody (HRP labeled) (1 : 2000, Immunoway, China) for 50 min at room temperature. Finally, after washing with PBS, the samples were dehydrated in an alcohol gradient and mounted using neutral gum for scanning.

### 2.5. Proteomics analysis

#### 2.5.1. Sample pretreatment

Biological replicates consisting of six males and six females from each cohort were used for quantitative analysis (48 samples in total). Pre-treatment of hippocampal protein samples and quantitative analysis of proteins were following the description of previous study [15].

#### 2.5.2. LC-MS quantitative proteomics analysis

Data-Independent Acquisition (DIA) proteomics analysis tests were performed using Thermo U3000nano RSLC ultra-high performance nanoliter liquid chromatography (Thermo Fisher Scientific, USA) in tandem with Orbitrap Fusion Lumos TM quadrupole-linear ion trap-electrostatic field orbitrap high-resolution mass spectrometry (MS) (Thermo Fisher Scientific, USA), and data acquisition was completed using the software XCalibur 4.3 (Thermo Fisher Scientific, USA).

The pre-treated samples were directly infused, ionized by electrospray, and the resulting peptide cations were separated in the gas phase before detection by DIA with high-resolution MS [16]. The main parameters of LC-MS DIA proteomics analysis are as follows. Chromatographic separation conditions: two Column Mode: Trap Column (Acclaim PepMap C18,  $3\mu\text{m}$ ,  $100\text{ \AA}$ ,  $75\mu\text{m} \times 2\text{ cm}$ ), Analytical Column

(Acclaim PepMap C18, 2 $\mu$ m, 100 Å, 75 $\mu$ m x 25 cm); mobile phase: A: 0.1 % Formic acid in water; B: 0.1 % Formic acid in 80 % Acetonitrile; Gradient: 3 % - 6 % B in 3 min, 8 % - 30 % B in 95 min, 30 % - 99 % B in 4 min, 99 % - 99 % B in 5 min; flow rate: 300 nL/min. Mass spectrometry detection conditions: spray voltage: 2.1 kV; capillary temperature: 300 °C; S-lens: 50 %; collision energy: 32 % HCD; resolution setting: full ms 60,000@ $m/z$  200, DIA scans 30,000@ $m/z$  200; Max IT: full MS 20 ms, full MS/MS 54 ms; parent ion scanning range:  $m/z$  350–1200; product ion scanning range: start from  $m/z$  200; number of windows: 80; Isolation window 10 Da.

### 2.5.3. Protein identification and quantitative analysis

Analysis was performed using Data Independent Acquisition (DIA) quantitative proteomics technique. Chromatogram library and Mouse\_Uniport (version 03, 2020) database were taken for protein identification in this study. DIA results were imported into Spectronaut 14 (Biognosys AG, Switzerland), targeted extracted with mouse chromatography library, meanwhile, the peptide and protein false discovery rate was strictly controlled < 1 % to obtain the final protein identification and quantitative information. Spectronaut 14 derives normalized protein intensity, this value was imported into Perseus (Max-Planck-Institute of Biochemistry, Germany) and Metaboanalyst (<https://www.metaboanalyst.ca>) for statistical analysis. FDR  $P$  value < 0.05 was used as the threshold value as differentially expressed proteins (DEPs).

### 2.5.4. Functional analysis of DEPs

The up-regulated and down-regulated DEPs were imported into webgestalt (<http://www.webgestalt.org/>) for GO and KEGG functional annotation and enrichment analysis, respectively. The GO and KEGG enrichment annotations were screened with FDR  $P$  value < 0.05, and the corresponding bar and bubble plots were drafted.

## 2.6. Lipidomic analysis

### 2.6.1. Sample pretreatment

Biological replicates consisting of six males and six females from each group were used for quantitative analysis (48 samples in total). The hippocampal tissue was homogenized using pre cooled methanol water extract (V/V, 8/2), centrifuged at 13000 g, 10 minutes for stratification, and the upper layer was lipid extract.

### 2.6.2. UPLC-HRMS Untargeted Lipidomic Analysis

Untargeted lipidomic analysis tests were performed using Ultimate 3000 ultra-high performance liquid chromatograph coupled with Q Exactive™ quadrupole-Orbitrap high resolution mass spectrometer UPLC-HRMS system (Thermo Scientific, USA). The main parameters of UPLC-HRMS Untargeted lipidomic analysis were as follows. Separation conditions for UPLC: metabolites were separated by using an Acquity TM HSS C18 column (Waters Co., USA, 2.1 × 100 mm), and eluted by 0.1 % formate/water and acetonitrile using linear gradient ramping from 2 % organic mobile phase to 98 % in 10 min. Furthermore, other mobile phases consisting of water and ammonium acetonitrile/methanol both containing ammonium bicarbonate buffer salt were employed to eluted metabolites separated on an Acquity TM BEH C18 column (Waters Co., USA, 1.7  $\mu$ m, 2.1 × 100 mm), the gradient was used as follow: 0 min 2 % organic phase ramped to 100 % in 10 min, and other 5 min was used for column washing and quilibrating. The flowrate, injection volume and column temperature were all set at the same conditions, 0.4 mL/min, 5  $\mu$ L and 50°C, respectively. Separation conditions for HRMS: the quadrupole-Orbitrap mass spectrometer was all operated under identical ionization parameters with a heated electrospray ionization source except ionization voltage including sheath gas 45 arb, aux gas 10 arb, heater temperature 355°C, capillary temperature 320°C and S-Lens RF level 55 %. The lipidomic analysis was profiled with full scan mode under 70,000 FWHM resolution with AGC 1E6 and 200 ms max injection time. 70–1000  $m/z$  scan range was acquired. Apex trigger,

dynamic exclusion and isotope exclusion was turned on, precursor isolation window as set at 1.0 Da. Stepped normalized collision energy was employed for collision induced disassociation of metabolite using ultra-pure nitrogen as fragmentation gas.

### 2.6.3. Lipid identification and quantification

Metabolic profiling data were further processed using Compound Discoverer (Thermo Scientific, USA) software. The area under the curve was extracted as quantitative information of the metabolites using XCalibur Quan Browser (Thermo Scientific, USA), and all peak area data of the labeled metabolites were exported to Excel software for collated post-statistical analysis (Microsoft, USA). Lipidomics data were processed using LipidSearch (Thermo Scientific, USA) software, the lipid identification was strictly manually checked and investigated one-by-one to eliminate false positive chiefly basing on peak shake, adduct ions behavior, fragmentation pattern, and chromatographic behavior. Lipids in the test with a corrected FDR  $P$  value < 0.05 were considered as differentially lipid metabolite.

### 2.6.4. Functional analysis of differential lipid metabolites

Metabolic pathway analyses were performed on the MetaboAnalyst website. The pathways enrichment annotations were screened with FDR  $P$  value < 0.05, and the corresponding bar and bubble plots were drafted.

## 2.7. Statistically analysis

Statistical analysis was performed using SPSS 22.0 software. Continuous variables were expressed as mean  $\pm$  standard deviation (mean  $\pm$  SD). Comparisons between groups were made using Student's  $t$ -test or one-way ANOVA.  $P$  < 0.05 indicates that the differences are statistically significant. Principal component analysis (PCA) was performed in soft independent modeling of class analogy (SIMCA) and clustering analysis was conducted in TB tools.

## 3. Results

### 3.1. Body weight and daily food intake of experimental animals

The body weight and its changes were summarized in Table 2, the body weight of mice in each group increased steadily during the intervention. The ApoE<sup>-/-</sup> mice showed slightly higher body weight than C57 mice, but the difference was not statistically significant. The average daily food consumption of mice in the four groups is shown in Fig. 1, and there is no statistical difference in the average daily dietary intake between the groups.

### 3.2. Cortical cholesterol level and cholesterol metabolism related molecule expression

As shown in Fig. 2A, ApoE<sup>-/-</sup> mice have higher cortical TC and LDL-C levels than C57 mice ( $P$  < 0.05). DHA intervention caused a significant decrease in cortical TC level in both ApoE<sup>-/-</sup> and C57 mice ( $P$  < 0.05). After DHA treatment, the cortical HDL-C level was down-regulated in

**Table 2**  
The body weight of experimental animals (g).

Intervention time	C57 mice		ApoE <sup>-/-</sup> mice	
	Control group	DHA group	Control group	DHA group
Baseline	24.19 $\pm$ 3.32	26.24 $\pm$ 4.65	27.19 $\pm$ 3.52	26.77 $\pm$ 3.22
The 5th month	26.53 $\pm$ 4.45	27.94 $\pm$ 5.70	28.13 $\pm$ 5.28	27.08 $\pm$ 3.40
Weight changes	2.33 $\pm$ 1.83	1.70 $\pm$ 4.92	0.94 $\pm$ 3.35	0.31 $\pm$ 1.23

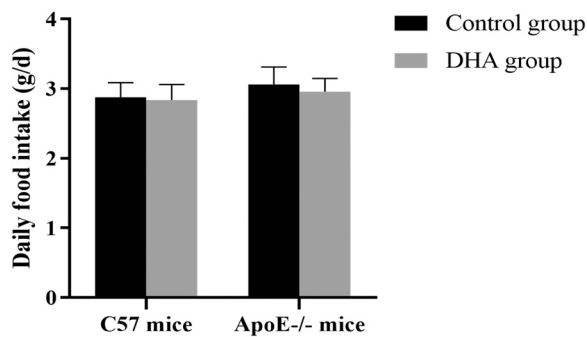


Fig. 1. Average daily food intake of experimental animals during the experimental period (g/d).

C57 mice, but up-regulated in ApoE<sup>-/-</sup> mice ( $P < 0.05$ ). The DHA treatment increased cortical LDL-C level in C57 mice, but a decrease of LDL-C in ApoE<sup>-/-</sup> mice ( $P < 0.05$ ).

As shown in Fig. 2B(a), in both cortex and hippocampus, LDLR protein expression in ApoE<sup>-/-</sup> mice was significantly higher than that in C57 mice ( $P < 0.05$ ). DHA treatment up-regulated cortical LDLR protein expression in C57 mice, but down-regulated the protein expression in ApoE<sup>-/-</sup> mice ( $P < 0.05$ ). After DHA treatment, LDLR protein expression in the hippocampal CA1 region was significantly up-regulated in ApoE<sup>-/-</sup> mice ( $P < 0.05$ ), but no change was observed in C57 mice ( $P > 0.05$ ). DHA treatment significantly down-regulated LDLR protein expression in the hippocampal CA3 region in C57wt mice ( $P < 0.05$ ), but did not affect the protein expression in ApoE<sup>-/-</sup> mice ( $P > 0.05$ ).

As shown in Fig. 2B(b), ApoE<sup>-/-</sup> mice displayed higher ABCG1 protein expression in cortex and hippocampal CA1 region than C57 mice ( $P < 0.05$ ). After DHA treatment, cortical and hippocampal ABCG1 protein expression was down-regulated in ApoE<sup>-/-</sup> mice, but only up-regulated the protein expression in the hippocampus CA3 region in C57 mice ( $P < 0.05$ ).

As shown in Fig. 2B(c), SORT1 protein expression in the hippocampal CA3 region was higher in C57 mice compared to ApoE<sup>-/-</sup> mice ( $P < 0.05$ ). In C57 mice, its expression was significantly up-regulated in cortex and was down-regulated in the hippocampal CA3 region after

DHA treatment. In ApoE<sup>-/-</sup> mice, a significant decrease was observed only in the hippocampal CA1 region, with no significant effect observed in the cortex and hippocampal CA3 region after DHA treatment ( $P > 0.05$ ).

As shown in Fig. 2B (d), in cortex and hippocampal CA1 region, the ApoE<sup>-/-</sup> mice showed similar expression of LOX1 protein as C57 mice, while, in hippocampal CA3 region, the ApoE<sup>-/-</sup> mice displayed much higher LOX1 protein expression than C57 mice ( $P < 0.05$ ). After DHA treatment, the expressions of LOX1 in the cortex and both hippocampus CA1 and CA3 were significantly up-regulated in C57 and ApoE<sup>-/-</sup> mice ( $P < 0.05$ ), and the increase was much more significant in ApoE<sup>-/-</sup> mice.

### 3.3. Bioinformatics analysis of DEPs

#### 3.3.1. Protein identification and DEPs screening

The principal component analysis (PCA) results showed that the hippocampal proteins of all groups were tightly clustered and did not overlap with the compared groups, indicating good intra group repeatability and high inter group discrimination (Fig. 3A). The differential proteins between groups were shown in Fig. 3B. Compared with C57 control mice, 10 proteins were down-regulated and 5 proteins were up-regulated in hippocampus in DHA treated C57 mice (Fig. 3C, D). The down-regulated proteins mainly function as regulator in apoptosis, inflammation, transmembrane signaling pathway, neurotransmitter release, vesicular trafficking processes and transport vesicle docking to the plasma membrane. The up-regulated proteins mainly participated in the modulation of ERK signaling pathway, synapse maintenance and neuronal survival, systemic glucose tolerance and insulin sensitivity, controlling of proteasome function, and functioning as membrane anchoring proteins to play a crucial role in sorting proteins into small extracellular vesicles.

Compared with C57 control mice, 10 proteins were down-regulated and 4 proteins were up-regulated in ApoE<sup>-/-</sup> control mice (Fig. 3C, D). The down-regulated proteins mainly involved in lipid metabolism, regulation of GTPase activity in neurons, neurite branching and motor neuron axon guidance, neural stem proliferation, transport of vesicle docking to the plasma membrane, and neurodevelopment. The up-regulated proteins mainly participated in aerobic glycolysis,

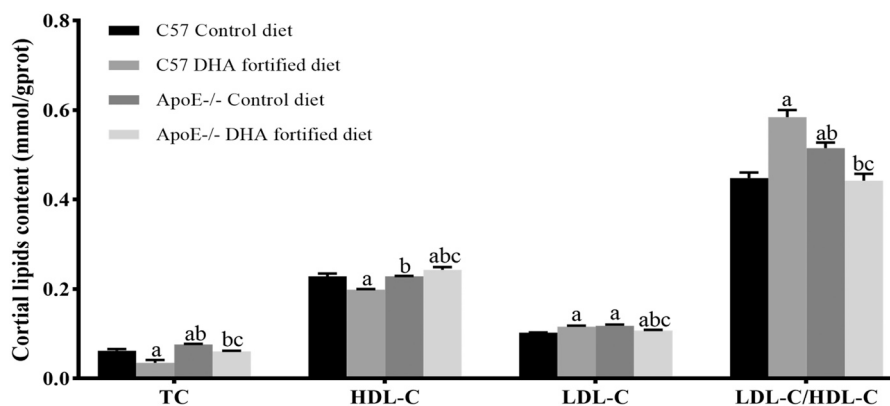


Fig. 2. A. Cortical lipid level in C57 and ApoE<sup>-/-</sup> mice treated with different diets. C57 and ApoE<sup>-/-</sup> mice were given a control diet or a DHA-fortified diet respectively for 5 months. Cortical TC, HDL-C, LDL-C levels were measured ( $n = 12$  for each group, six males and six females), and calculate the ratio of LDL-C to HDL-C. Data are expressed as mean  $\pm$  SD. a:  $P < 0.05$  compared with the control diet-fed C57 mice; b:  $P < 0.05$  compared with the DHA-fortified diet-fed C57 mice; c:  $P < 0.05$  compared with the control diet-fed ApoE<sup>-/-</sup> mice. B. Cortical and hippocampal expression of lipid metabolism-related molecular protein in C57 and ApoE<sup>-/-</sup> mice. Cortical expression of lipid metabolism-related molecular proteins in C57 and ApoE<sup>-/-</sup> mice were given a control diet or a DHA-fortified diet for five months. The expression of lipid metabolism-related molecules were measured ( $n = 12$  for each group, six males and six females). Data are expressed as mean  $\pm$  SD. (a) LDLR protein expressions in cortex from C57 and ApoE<sup>-/-</sup> mice treated with different diets. (b) The expression of ABCG1 protein in cortex and hippocampus from C57 and ApoE<sup>-/-</sup> mice treated with different diets. (c) The expression of SORT1 protein in cortex and hippocampus from C57 and ApoE<sup>-/-</sup> mice treated with different diets. (d) The expression of LOX1 protein in cortex and hippocampus from C57 and ApoE<sup>-/-</sup> mice treated with different diets. Scale bar: 50  $\mu$ m. The bar charts are quantitative results for the representative images on the left, respectively. Data are expressed as mean  $\pm$  SD. a:  $P < 0.05$  compared with the control diet-fed C57 mice; b:  $P < 0.05$  compared with the DHA-fortified diet-fed C57 mice; c:  $P < 0.05$  compared with the control diet-fed ApoE<sup>-/-</sup> mice.

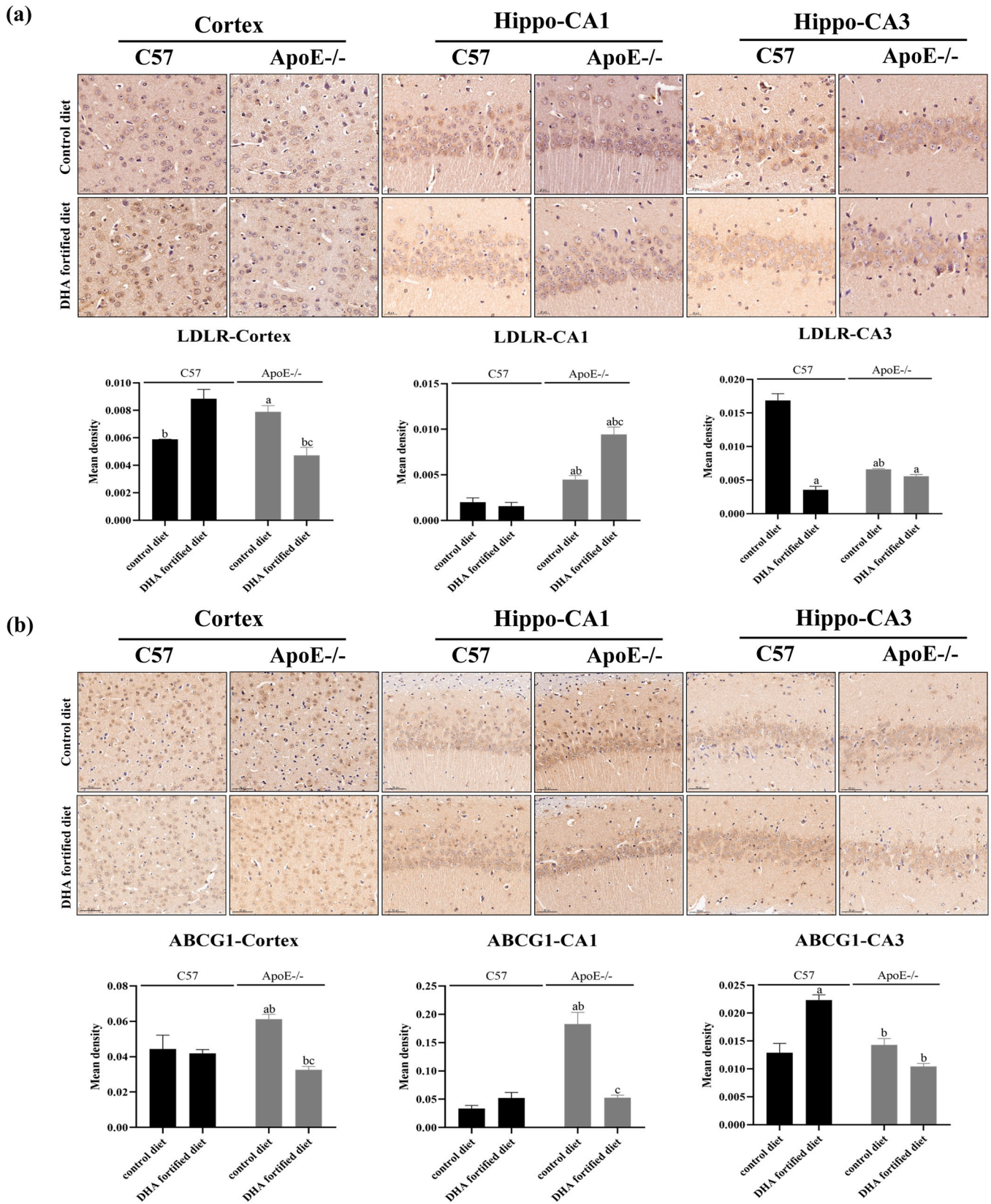


Fig. 2. (continued).

antioxidant activity, neural development, and maintaining immune self-tolerance, synaptic function and lipid and energy homeostasis.

Compared with DHA treated C57 mice, 18 proteins were down-regulated, and 13 proteins were up-regulated in DHA treated ApoE<sup>-/-</sup>

mice (Fig. 3C, D). The down-regulated proteins mainly involved in cholesterol metabolism, inflammatory response, the formation or maintenance of the myelin, brain sugar transport and the formation of synapse. The up-regulated proteins mainly participated in intracellular

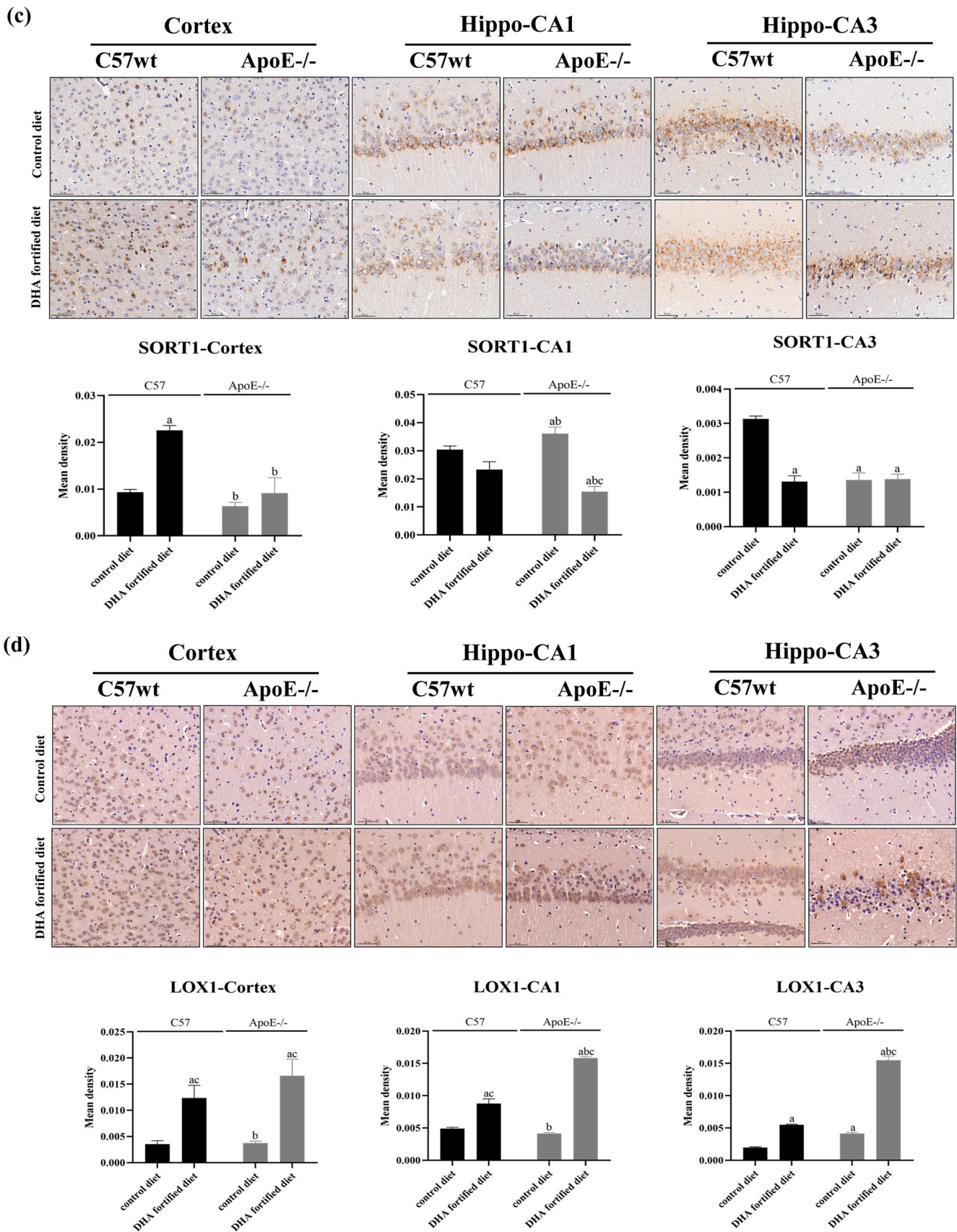
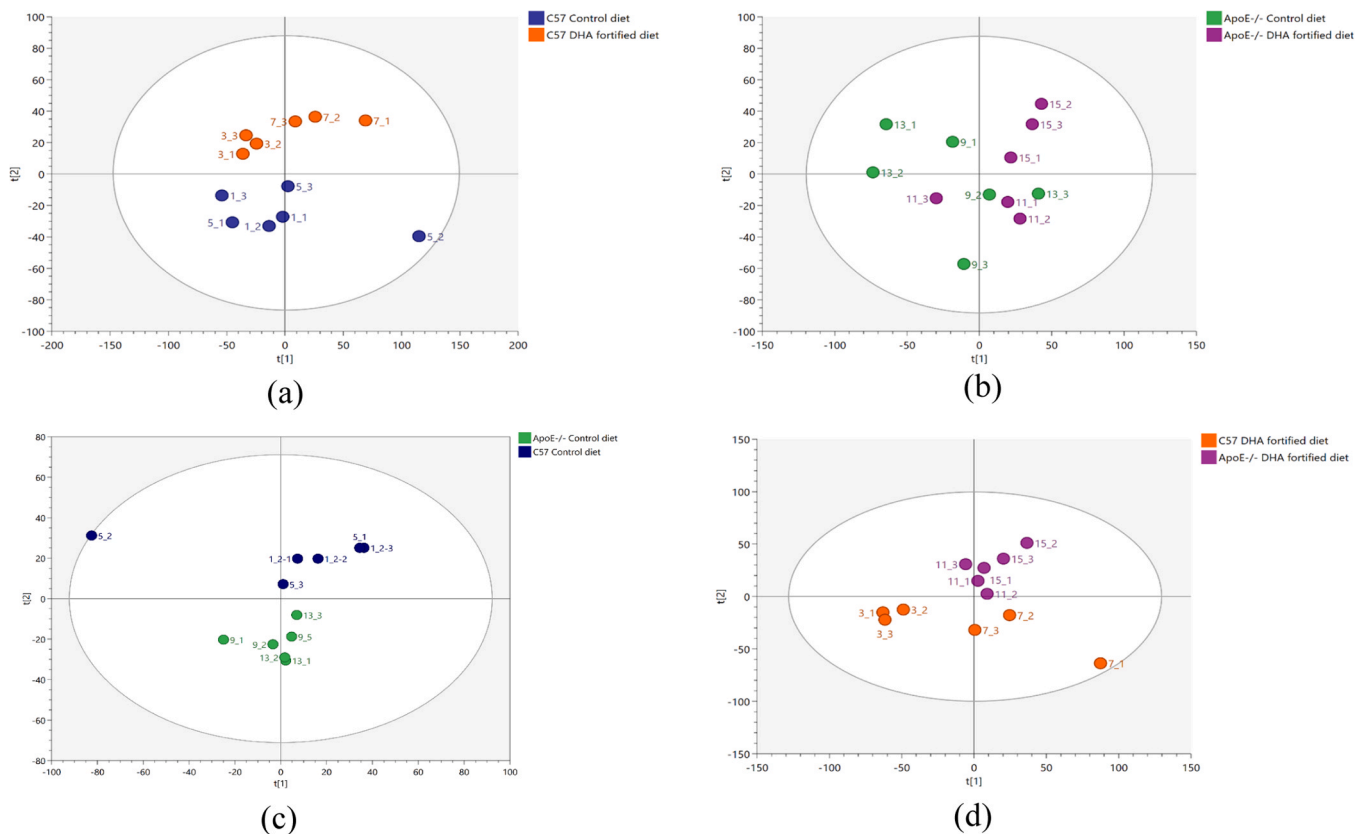


Fig. 2. (continued).



**Fig. 3. A. PCA score of differentially proteins.** Data-Independent Acquisition proteome data is logarithmically transformed and modeled according to Pareto ratio. Figures indicate the comparison of DHA intervention group vs control group in C57 mice (a) and ApoE-/- mice (b), respectively; ApoE-/- group vs C57 group in both feeding with control diet (c) and DHA fortified diet (d), respectively. **B. Volcano map of differentially proteins.** The horizontal coordinate of the volcano plot is  $\log_2$  (fold change), and the vertical coordinate is  $-\log_{10}$  (FDR  $P$  value), the further away from the 0 points the greater the difference. Up-regulated proteins are on the right side, down-regulated proteins are on the left side, down-regulated differentially expressed proteins are indicated by green dots, up-regulated differentially expressed proteins are indicated by orange dots, and non-significant differentially expressed proteins are indicated by gray dots, and the labels are the names of the genes corresponding to the differentially expressed proteins. (a), (b), (c) and (d) indicate the comparison of C57 DHA intervention group and C57 control group, ApoE-/- DHA intervention group and ApoE-/- control group, and ApoE-/- control group and C57 DHA intervention group, respectively. **C. Bar chart of differentially proteins.** The bar of different colors correspond to the expression of differential proteins, and the height of the bar represents the amplitude of fluctuations.  $\log_2$ Fold Change  $< 0$  indicates down-regulated protein, while  $\log_2$ Fold Change  $> 0$  indicates up-regulated protein. Figures (a), (b), and (c) show the comparison between C57 DHA intervention group and C57 control group, ApoE-/- control group and C57 control group, ApoE-/- DHA intervention group and C57 DHA intervention group, respectively. **D. Heat map of clustering of differential protein patterns.** The different colors in the upper right legend correspond to the expression of the differential protein, red indicates up-regulation of the differential protein, blue indicates down-regulation of the differential protein, and the shade of color represents the magnitude of up-regulation. (a), (b) and (c) indicate the comparison of C57 DHA intervention group and C57 control group, ApoE-/- control group and C57 control group, ApoE-/- DHA intervention group and C57 DHA intervention group, respectively. **E. Bar chart of GO enrichment classification of differentially proteins.** Blue, red, and green bars represent biological processes, cellular components, and molecular functions, respectively. (a), (c), and (e) are up-regulated protein GO enrichment classification bars, (b), (d), and (f) are down-regulated protein enrichment classification bars, (a) and (b), (c) and (d), as well as (e) and (f) represent C57 DHA intervention group and C57 control group, ApoE-/- control group and C57 control group, ApoE-/- DHA intervention group and C57 DHA intervention group, respectively. **F. Differential protein KEGG enrichment bubble map.** The horizontal coordinate is  $\log_2$  ER and the vertical coordinate is the name of the signaling pathway. KEGG signaling pathways with significant enrichment of differential proteins were selected based on the criterion of FDR  $P$  value  $< 0.05$ . (a) is the comparison of up-regulated differential proteins between ApoE-/- control group and C57 control group, and (b) is the comparison of down-regulated differential proteins between ApoE-/- DHA intervention group and C57 DHA intervention group. (For interpretation of the references to color in this figure legend, the reader is referred to the web version of this article.)

esterification of lipid acids, regulation of cell growth, acidifying the extracellular environment, and TGF-beta signaling pathway.

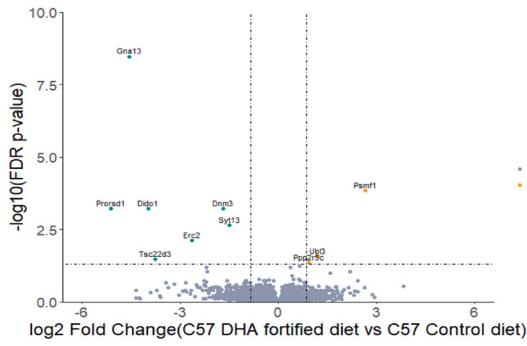
### 3.3.2. GO enrichment analysis of DEPs

By GO analysis, a total of 10 DEPs in the C57 DHA group versus the C57 control group were classified into 26 significant GO terms in biological processes, cellular components, and molecular functions (Fig. 3E). Notably, four proteins were found to be associated with energy metabolic processes, including the process of phospho-pentose metabolism, metabolic regulation of NADP, the process of glucose-3-phosphate metabolism, and secondary metabolic processes.

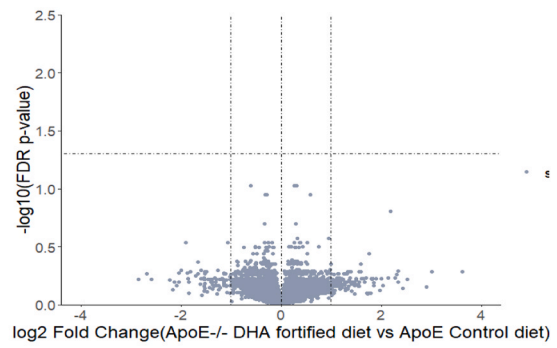
Compared with C57 control mice, DEPs have mainly undergone

changes in biological processes, cellular components, and molecular functions in ApoE-/- control mice (Fig. 3E). The up-regulated proteins mainly involved in biological processes, such as cellular communication, cellular component organization, bioregulation, metabolism, and stimulatory responses, mainly involving in the regulation of hydrolase and transferase activities.

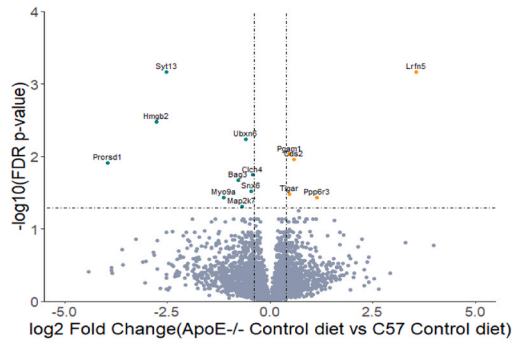
Compared with DHA fortified diet-fed C57 mice, the DEPs in DHA fortified diet-fed ApoE-/- mice mainly involved in biological processes, cellular components, and molecular functions (Fig. 3E). Both the up-regulated and down-regulated proteins participated in the regulation of enzyme activity and protein binding.



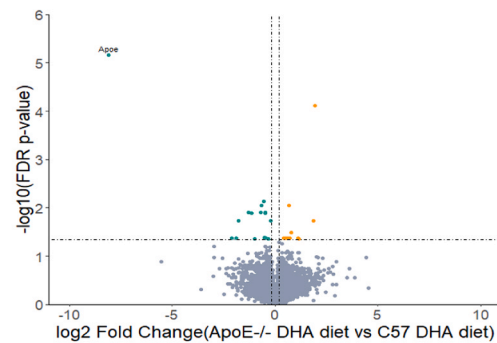
(a)



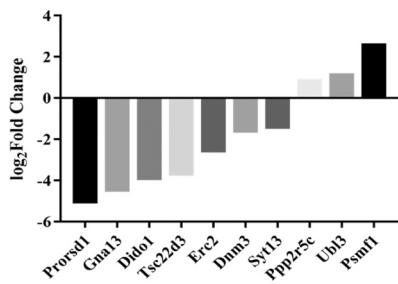
(b)



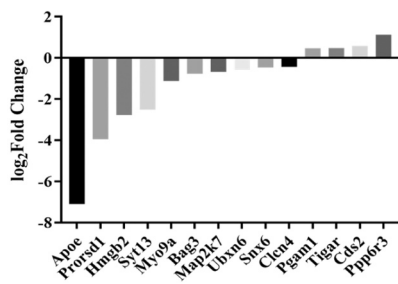
(c)



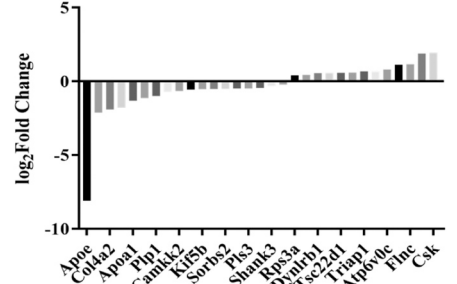
(d)



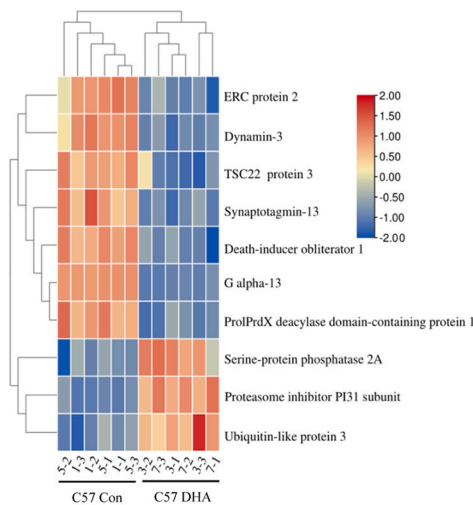
(a) C57 DHA and C57 con



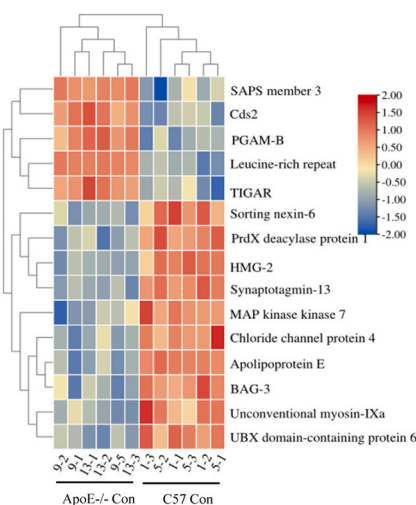
(b) ApoE<sup>-/-</sup> con and C57 con



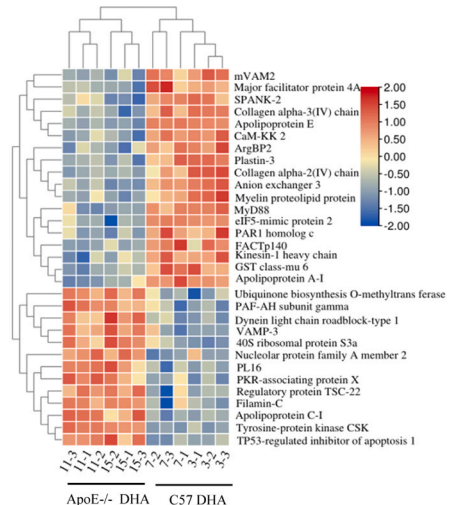
(c) ApoE<sup>-/-</sup> DHA and C57 DHA



(a)



(b)



(c)

Fig. 3. (continued).

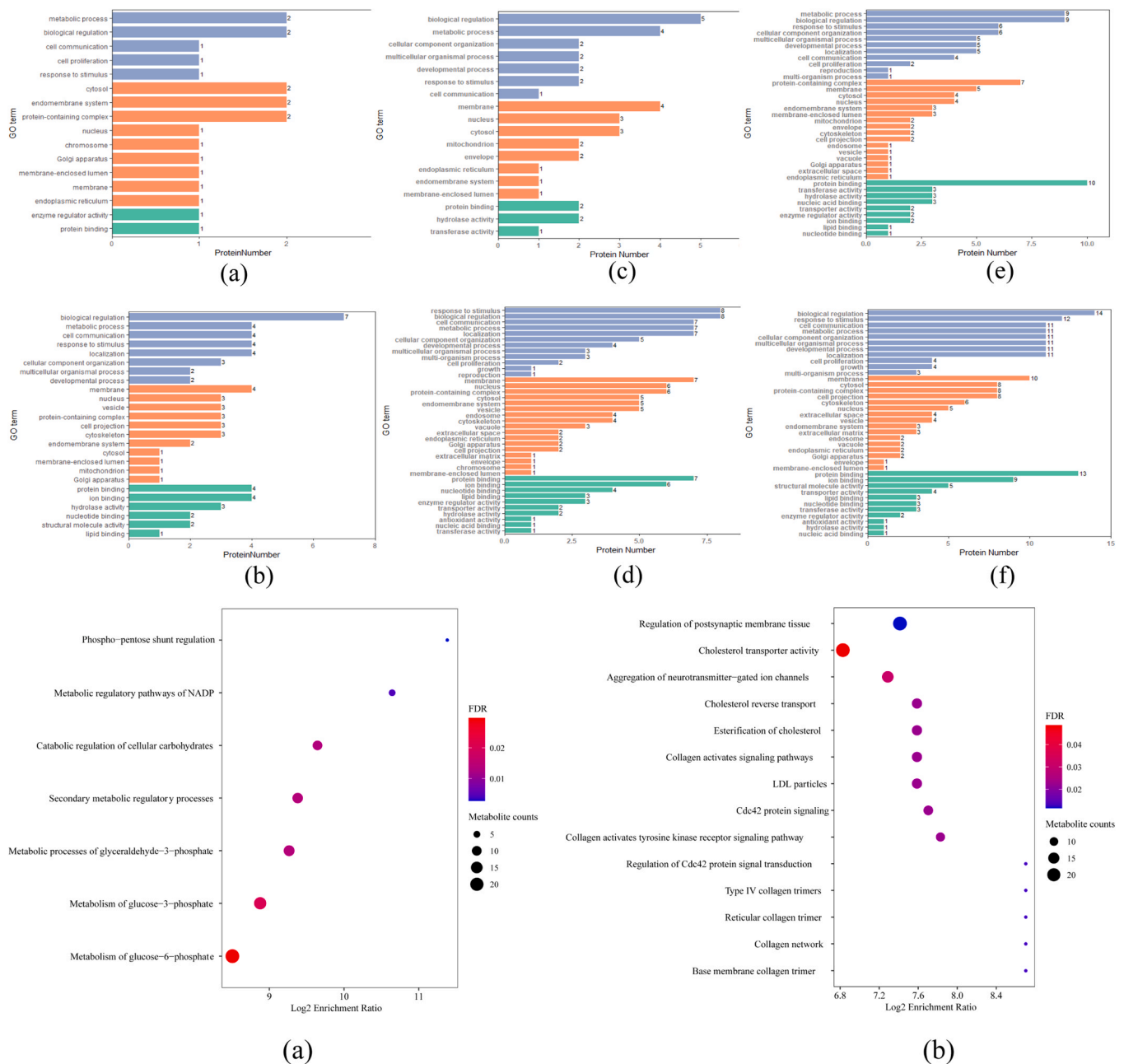


Fig. 3. (continued).

### 3.3.3. Enrichment analysis of differentially expressed protein KEGG

Six enriched pathways were identified by KEGG in the ApoE-/- control group versus the C57 control group and 14 enriched pathways in the C57 DHA intervention group versus the ApoE-/- DHA intervention group with statistically significance ( $P < 0.05$ ) (Fig. 3F). Six energy metabolism pathways (phosphate-pentose shunt regulation, metabolic regulatory pathway of NADP, metabolic process of glucose-3-phosphate, and secondary metabolic regulatory process) and three collagen metabolic pathways (collagen network, collagen activation signaling pathway, and collagen-activated tyrosine kinase receptor signaling pathway) were identified.

### 3.4. Bioinformatics analysis of differential lipidomic metabolites

#### 3.4.1. Lipid identification and differential lipid metabolites screening

The principal component analysis (PCA) results showed that the hippocampal lipid metabolites of all groups were tightly clustered and

did not overlap with the compared groups, indicating good intra group repeatability and high inter group discrimination (Fig. 4A). The differential lipids between groups were shown in Fig. 4B, and differential lipids were not found in ApoE-/- control mice versus C57 control mice. The common differential lipids in each group are shown in the Figs. 4C and 4D, and the significantly different lipid metabolites among groups are phosphatidylcholines (PC) and phosphatidylethanolamines (PE). Compared with C57 control mice, 50 lipids were down-regulated and 80 lipids were up-regulated in hippocampus in DHA treated C57 mice (Fig. 4E). The lipids that undergo changes were mainly related to the metabolism of glycerophospholipids, accounting for more than 50 % of the total differential lipids, especially phosphatidylethanolamine and phosphatidylcholine.

Compared with ApoE-/- control mice, 66 lipids were down-regulated and 75 lipids were up-regulated in ApoE-/- DHA mice (Fig. 4E). Differentially lipid classes that underwent changes were similar to those of the previous comparator group, with the majority involved in

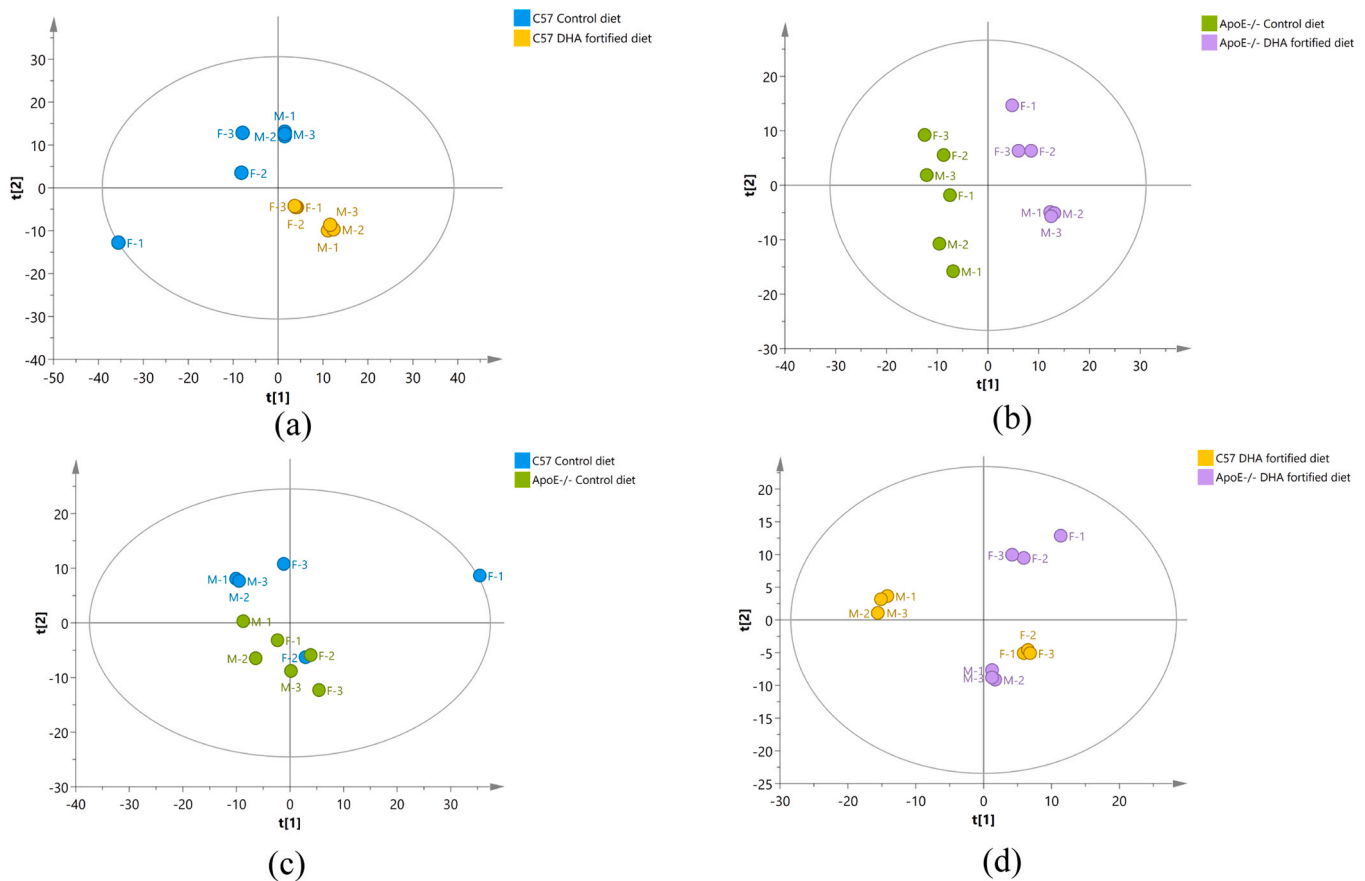


**Fig. 4. A. PCA score of differentially lipid metabolites.** Data-Independent Acquisition proteome data is logarithmically transformed and modeled according to Pareto ratio. Figures indicate the comparison of DHA intervention group vs control group in C57 mice (a) and ApoE<sup>-/-</sup> mice (b), respectively; ApoE<sup>-/-</sup> group vs C57 group in both feeding with control diet (c) and DHA fortified diet (d), respectively. **B. Volcano map of differentially lipid metabolites.** The horizontal coordinate of the volcano plot is  $\log_2$ (fold change), and the vertical coordinate is  $-\log_{10}$ (FDR  $P$  value), the further away from the 0 points the greater the difference. Up-regulated lipids are on the right side, down-regulated lipids are on the left side, down-regulated differentially lipids are indicated by green dots, up-regulated differentially lipids are indicated by pink dots, and non-significant differentially lipids are indicated by blue dots. (a), (b), (c) and (d) indicate the comparison of C57 DHA intervention group and C57 control group, ApoE<sup>-/-</sup> DHA intervention group and ApoE<sup>-/-</sup> control group, and ApoE<sup>-/-</sup> control group vs C57 DHA intervention group, respectively. **C. Venn diagram and bar chart of differential metabolites.** (a) The three coloured ovals represent the three comparison groups and the numbers are the number of identical differential lipids in each comparison group. (b) The bar of different colors correspond to the expression of differential lipids, and the height of the bar represents the amplitude of fluctuations.  $\log_2$ Fold Change < 0 indicates down-regulated protein, while  $\log_2$ Fold Change > 0 indicates up-regulated protein. PC, Phosphatidylcholine; PE, Phosphatidylethanol. (c) The height of the bars represents the number of differential metabolites. Comparisons of the C57 DHA intervention group with the C57 control group, the ApoE<sup>-/-</sup> DHA intervention group with the ApoE<sup>-/-</sup> control group, and the ApoE<sup>-/-</sup> DHA intervention group with the C57 DHA intervention group are shown. **E. Heat map of clustering of differential metabolites.** The different colors in the upper right legend correspond to the expression of the differential metabolite, red indicates up-regulation of the differential metabolite, blue indicates down-regulation of the differential metabolite, and the shade of color represents the magnitude of up-regulation. (a), (b) and (c) indicate the comparison of C57 DHA intervention group and C57 control group, ApoE<sup>-/-</sup> DHA intervention group and ApoE<sup>-/-</sup> control group, ApoE<sup>-/-</sup> DHA intervention group and C57 DHA intervention group, respectively. **F. KEGG enrichment bubble map of differential metabolites.** The horizontal coordinate is  $\log_2$  ER and the vertical coordinate is the name of the signaling pathway. KEGG signaling pathways with significant enrichment of differential metabolites were selected on the criterion of FDR  $P$  value < 0.05. (a), (b) and (c) indicate the comparison of C57 DHA intervention group and C57 control group, ApoE<sup>-/-</sup> DHA intervention group and ApoE<sup>-/-</sup> control group, ApoE<sup>-/-</sup> DHA intervention group and C57 DHA intervention group, respectively. (For interpretation of the references to color in this figure legend, the reader is referred to the web version of this article.)

glycerophospholipid metabolism, accounting for 74 % of up-regulated lipids and 80 % of down-regulated lipids. Compared with DHA treated C57 mice, 14 lipids were down-regulated, and one lipid was up-regulated in DHA treated ApoE<sup>-/-</sup> mice (Fig. 4E). The differential lipids mostly belong to the broad categories of fatty acyl carnitines, PC and PE. Differential lipids were not found in the ApoE<sup>-/-</sup> control mice compared to the C57 control mice.

### 3.4.2. Enrichment analysis of differentially lipid by KEGG

9, 8, 3, and 26 enriched pathways were identified respectively by KEGG in the four comparison groups with statistically significance ( $P < 0.05$ ) (Fig. 4F). The metabolic pathways enriched to are mostly related to fatty acid (linoleic acid, alpha-linolenic acid, arachidonic acid)

metabolism, biosynthesis of unsaturated fatty acids, and phospholipid (glycerophospholipid and glycerolipid) metabolism.

## 4. Discussion

Our data indicated discrepant response of brain lipids and protein profile to DHA dietary intervention in C57 and ApoE<sup>-/-</sup> mice. Cholesterol is one of the major components of cell membranes, and impaired cholesterol homeostasis can cause AD [9], and increased neuron membranes cholesterol content was observed in the brain of AD patient [17]. Consistently, our results demonstrated elevated TC and LDL-C levels in ApoE<sup>-/-</sup> control mice as comparing with C57 control mice, implying abnormal brain cholesterol metabolism in ApoE defect mice. ApoE

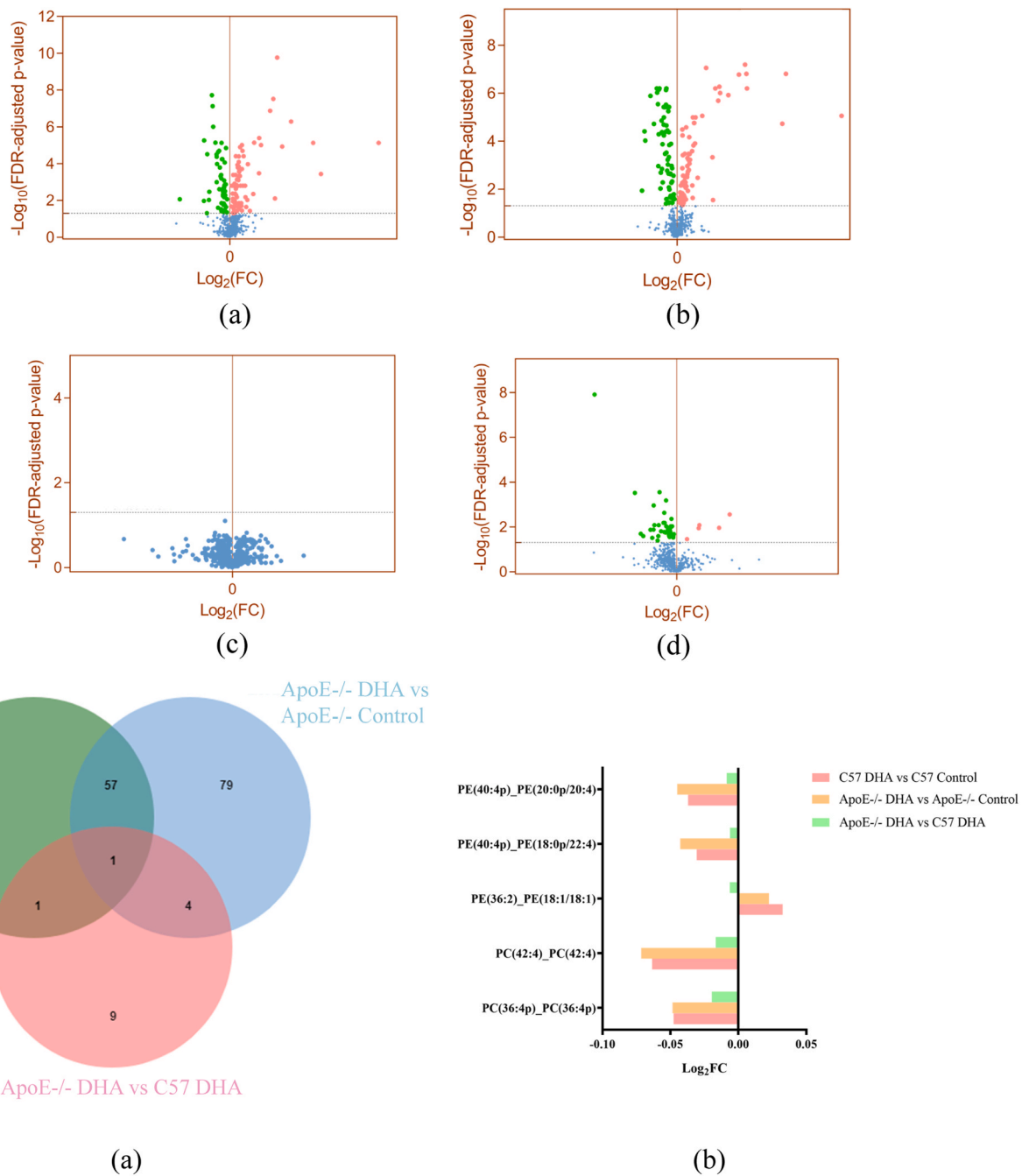


Fig. 4. (continued).

status-dependent regulating effects of DHA treatment on cortical cholesterol level were also demonstrated by opposite changes of cortical HDL-C, LDL-C levels and LDL-C/HDL-C ratio in DHA-fed C57 and ApoE<sup>-/-</sup> mice. All these data suggested the important role of ApoE in affecting cholesterol metabolism and in modifying the response of cerebral cholesterol metabolism to DHA intervention.

We found that the ApoE<sup>-/-</sup> mice showed relative higher cortical LDLR protein expression than C57 mice. It is reported that, due to lipoprotein clearance defects, ApoE<sup>-/-</sup> mice displayed higher level of residual lipoproteins [18]. Therefore, there is a compensatory response to abnormal cholesterol level caused by ApoE defect, and the increase in LDLR expression might mediate the clearance of LDL-C and remnant lipoproteins from the circulation, thereby maintaining normal cholesterol level. DHA intervention reduced hippocampal LDLR expression in both ApoE<sup>-/-</sup> and C57 mice, which might be attributable to the

beneficial effects of DHA on maintaining brain cholesterol metabolism in a normal status, and reducing brain neuropathy [19].

It has been shown that ABCG1 mediated cholesterol efflux levels are reduced in the absence of ApoE [20]. ApoE<sup>-/-</sup> mice maintain brain lipid homeostasis by increasing ABCG1 levels so that excess lipids will be removed via reverse cholesterol transport [21]. Study found that ABCG1-mediated cholesterol efflux pathway and the size of the cellular free cholesterol pool will be significantly increased after DHA intervention [22]. Our data indicated that defect in the ApoE could alter the response of brain ABCG1 expression to DHA treatment, as evidenced by a significant reduction in DHA-fed ApoE<sup>-/-</sup> mice. In ApoE<sup>-/-</sup> mice, increased cortical ABCG1 protein expression suggests a link between ApoE status and ABCG1-dependent cholesterol efflux in influencing cerebral lipid metabolism [23]. Collectively, these results indicate that the absence of ApoE may affect brain lipid metabolism, and modify the

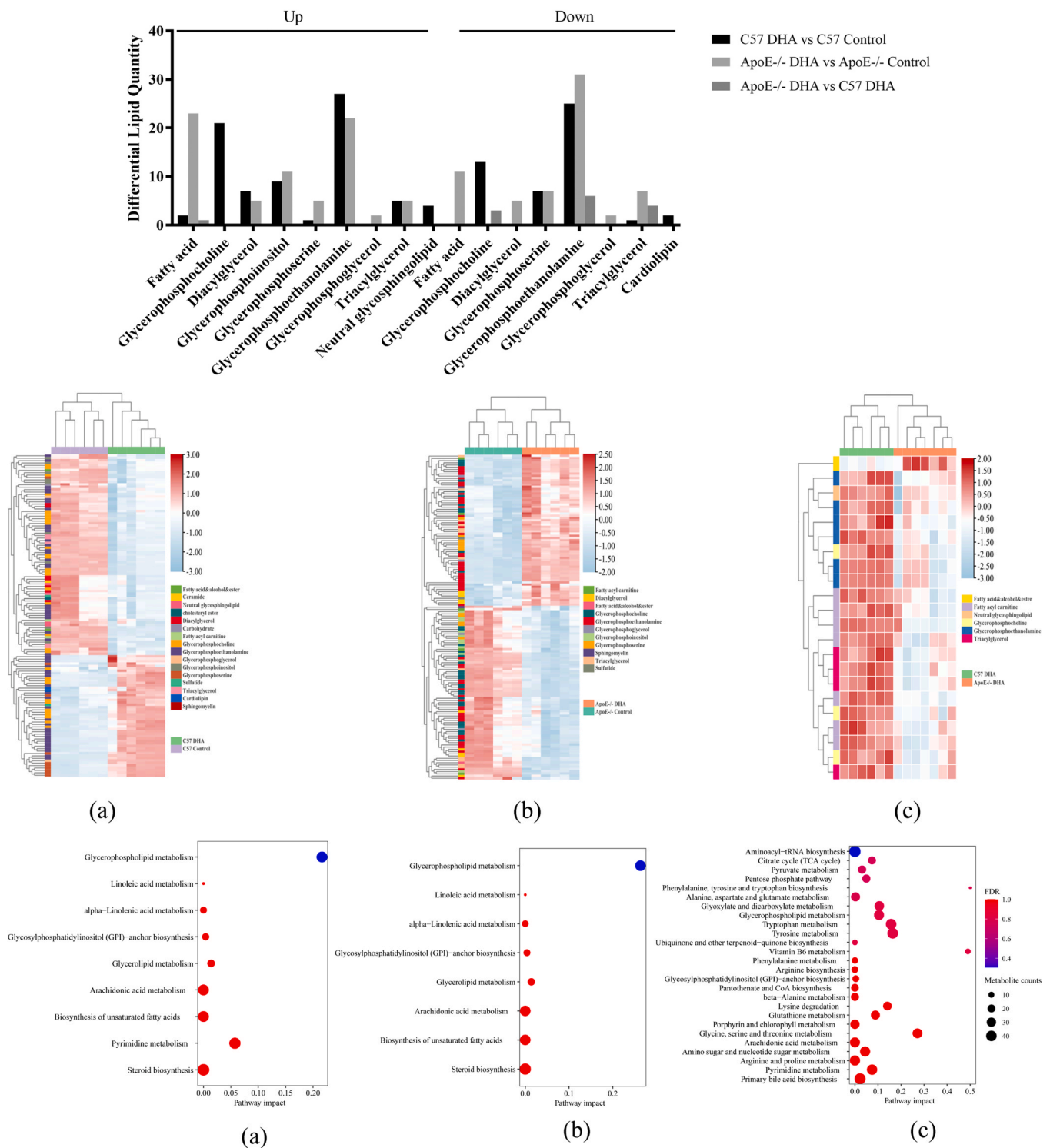


Fig. 4. (continued).

outcomes of DHA intervention in ApoE<sup>-/-</sup> mice.

Study in rodents has shown that SORT1 can bind extracellular ApoE/A $\beta$  complexes, delivering them to the lysosome for degradation [24]. Our data show that SORT1 protein expression is significantly increased only in the hippocampal CA1 region in ApoE<sup>-/-</sup> mice. We speculate that the hippocampal CA1 region is the susceptible and sensitive domain to have alteration of SORT1 expression in ApoE<sup>-/-</sup> mice. A study found that, in the absence of ApoE protein, SORT1 is unable to scavenge A $\beta$ , resulting in enhanced susceptibility to cognitive impairment in ApoE<sup>-/-</sup>

mice. Moreover, a significantly increased level of SORT1 was observed in the postmortem brain of AD patients [25]. These data further demonstrated the linkage between cerebral ApoE and SORT1 with the pathology of AD. In the current study, a dramatic decrease in SORT1 was found after DHA treatment in hippocampal CA1 region in ApoE<sup>-/-</sup> mice, indicating the impact of DHA on antagonizing ApoE defect-mediated SORT1 overexpression. We also observed discrepant cortical and hippocampal SORT1 expression after DHA treatment between C57 and ApoE<sup>-/-</sup> mice. These results further hint an ApoE-dependent regulating

effect of DHA on cerebral SORT1 expression in mice.

It was reported that oxygen LDL (ox-LDL) and caveolae are involved in the LOX1 expression, and LOX1 activity depends largely on the intact caveolae system [26]. Previous study has shown the ApoE-dependent modulation effect of DHA on caveolae activity, and due to a decrease in caveolin activity, knocking out of ApoE gene leads to a weakened role of DHA in maintaining vascular wall homeostasis [27]. In the current study, we found that DHA intervention displayed an extensively regulating effect on cortical and hippocampal LOX1 expression in both C57 and ApoE<sup>-/-</sup> mice. It is reported that DHA treatment significantly alters the microenvironment of the caveolae by changing the membrane lipid composition, resulting in the enhancement of the signaling pathway involved in the expression of LOX1 [28]. Additionally, the ApoE-dependent regulatory effect of DHA on cerebral LOX1 expression observed in our study was demonstrated by a much more significant increase of cortical and hippocampal LOX1 expression in ApoE<sup>-/-</sup> mice than in C57 mice. These data indicated that cerebral LOX1 protein expression was more sensitive to DHA treatment, hinting that LOX1 might be an efficient molecular target for DHA to regulate brain cholesterol metabolism in ApoE<sup>-/-</sup> mice.

In C57 mice, totally 7 differential proteins were identified after DHA dietary intervention, among them, three differential proteins, including dynamin-3(Dnm3), Synaptotagmin-13 (Syt13) and Ubiquitin-like protein 3 (Ubl3), mainly involved in vesicular trafficking processes and transport of vesicle. As a member of the dynamin superfamily, Dnm3 could provide the structural basis for proteins to perform a variety of basic cellular functions, such as the release of transport vesicles and cell division [29]. Normally, sterols and related lipids move between cells through vesicular and non-vesicular pathways in order to maintain intracellular lipid homeostasis [30]. In our study, we found that Dnm3 is down-regulated in the DHA-fed C57 mice compared to C57 control mice, suggesting that DHA intervention may play a crucial role in modulating the release of intracellular transport vesicle and reducing intercellular lipid exchange. Ubl3 is a ubiquitin-like protein (UBL), which was reported to be a post-translational modification factor in promoting protein sorting to small extracellular vesicles (sEVs) [31]. Proteins, lipids, RNA and DNA contained in sEVs can be horizontally transferred to recipient cells to promote cell-to-cell communication [32]. Recent study has demonstrated the relation between sEVs and neurodegenerative diseases [33]. Moreover, neurodegenerative disease-related molecules A $\beta$  is also annotated as UBL3-interacting protein [34], further demonstrating the involvement of UBL3 in sEV-related diseases. In our study, DHA-treated C57 mice showed an up-regulation of UBL3, suggesting that UBL3 might be a potential therapeutic target of DHA on affecting sEV-related neurodegenerative disease. Syt13 is another membrane trafficking protein that regulating intracellular vesicle exocytosis and movement. Study has found that Syt13 is mainly expressed in neuron that possesses regulatory secretory pathway, which produce and secrete hormones to regulate different systematic processes such as metabolism [35]. Although, increased Syt13 mRNA expression was observed in several brain regions after contextual fear conditioning, the exactly function of this protein in affecting neuron physiology is still unclear. In the current study, DHA treatment increased Syt13 expression in C57 mice. Moreover, comparing with C57 control mice, down-regulated Syt13 was also observed in ApoE<sup>-/-</sup> control mice. Given the important role of Syt13 in transporting vesicle docking to the plasma membrane [36], we speculated that ApoE and DHA might targeted Syt13 to modifying the physiological and pathological processes in neurons. Proteasome inhibitor PI31 subunit (Psmf1) was reported to play an important role in control of proteasome function, and is required for protein homeostasis, synapse maintenance, and neuronal survival [37]. The impacts of DHA on suppressing the deterioration of brain function, delaying the onset and progression of neurological disease has been reported by previous study [38]. These data indicated that the Psmf1 might be a mediator for DHA to exhibit neuroprotection.

Our data showed that, except of ApoE protein, ApoE defect caused

significant down-regulation of Prorsd1, Hmgb2 and Syt13 protein as comparing with C57 control mice. To date, the biological function of Prorsd1 is still less studied and characterized. It is interesting to find that DHA treatment also caused dramatically reduction of Prorsd1 protein in hippocampus, hinting the potential role of Prorsd1 in affecting neuron function as well as the outcomes of DHA intervention on brain. As one of the HMGB domain proteins, Hmgb2 was reported to participate in the transcription processes, regulation of the chromatin structure, cell differentiation, and activation of AKT signaling pathway [39]. Additionally, Hmgb2 interacts with steroid hormones (estrogen, androgen and glucocorticoid) and NLRP3 to regulate steroid hormone and inflammatory NF- $\kappa$ B signaling [40]. ApoE deficiency or abnormal ApoE status-mediated inflammation and neuron apoptosis have been reported by previous studies [41]. In the current study, the significantly down-regulated Hmgb2 protein in ApoE<sup>-/-</sup> mice further indicated the involvement of Hmgb2 in ApoE defect -medicated various cerebral pathological damage.

We found that the DHA intervention resulted in significant changes in the expression of diverse proteins in the hippocampus of ApoE<sup>-/-</sup> mice and C57 mice. The functional analysis of the differential proteins revealed that most of these proteins function related to bioregulation for stimulation response, and metabolism. The main functions of the up-regulated proteins mainly participated in hydrolase and transferase activity regulation, and protein or ion binding. The down-regulated proteins mainly involved in the binding action of various biomolecules, structural molecular activity, and enzyme activity regulation.

A well balance between saturated and unsaturated lipids is crucial for maintaining normal cellular function, and excessive deposition and metabolic abnormalities of fatty acids can cause lipotoxicity [42]. The results of GO analysis indicated that several proteins involved in the regulation of hydrolase activities were up-regulated in the hippocampus of DHA-fed ApoE<sup>-/-</sup> mice as compared with the C57 mice. One of them is adiponectin receptor2 (AdipoR2), which helps to remove saturated fatty acid from ceramide and can support normal membrane function under acute lipotoxic stress [43]. A study conducted by Tonnac et al. found that dietary DHA intake significantly increased the activity of hydrolases, thereby altering the occurrence of lipid metabolic-related molecular events and maintaining membrane lipid homeostasis [44]. These data were in line with our results, suggesting that the regulation of lipids metabolism-related enzymes might contribute to DHA-mediated neuron protective effects.

Additionally, we found a down-regulation of antioxidant activity-related proteins in ApoE<sup>-/-</sup> control mice compared to C57 control mice, suggesting that oxidative stress is one of potential target for ApoE gene defect-mediated neuron injury. Due to lower antioxidant active substances, ApoE<sup>-/-</sup> mice were reported to be more susceptible to oxidative stress as comparing with the controls [45]. However, ApoE<sup>-/-</sup> mice consistently showed down-regulation of antioxidant active protein compared with C57 mice after DHA intervention. We also found that DHA -fed ApoE<sup>-/-</sup> mice showed similar hippocampal protein profile as the control diet-fed ApoE<sup>-/-</sup> mice. A study found that carriers with ApoE4 genotype are more sensitive to DHA deficiency, and the deletion of ApoE might decrease cerebral DHA uptake [46]. We therefore speculate that the observed outcomes might attribute to reduced or inadequate DHA transport into the brain due to ApoE defect during short interventional period [47].

Additionally, the differential proteins in hippocampus between ApoE<sup>-/-</sup> and C57 mice were mainly focused on metabolism-related pathways, including glucose, lipid, and NADP metabolism pathways. Impaired metabolism of glucose was observed in 5 $\times$ FAD mice, and this metabolic deficiency was reported to be caused by metabolic reprogramming of glycolysis [48]. In our study, the abnormal glucose and lipid metabolism observed in ApoE<sup>-/-</sup> mice suggested ApoE dysfunction-mediated metabolic dysfunctions in brain.

After DHA intervention, 6 out of the 14 pathways enriched to KEGG were associated with collagen. Study has found that DHA activates

hippocampal collagen and collagen-related receptors in mice, thus reducing the damage caused by ApoE defect [49]. It was reported that, in ApoE<sup>-/-</sup> mice, the atherosclerotic plaques are prone to be disrupted by decreasing collagen deposition in aortic plaques and that adverse cardiovascular events occur as a result [50]. These results partially explain the increased risk of cerebrovascular disease in subjects with abnormal ApoE status. Decreased collagen deposition may contribute to the AD-related pathological changes in ApoE<sup>-/-</sup> mice. Study found that the biological activity of collagen weakened the toxicity of A $\beta$ , which may be affected by the cell-collagen interaction [51]. In addition to reducing the toxicity of A $\beta$ , collagen can also reduce the aggregation rate of A $\beta$  and inhibit the pathological process of AD.

Disorder of lysine, hydroxylysine and tryptophan metabolism was reported to cause the change of glutaryl carnitine level in body fluids and tissues, especially in the central nervous system [52]. Moreover, irreversible neurological injury caused by lysine metabolism disorder has also been reported by previous study [53]. Additionally, studies have found the participation of asparagine and aspartyl residues in post-translational modifications of amyloidogenic proteins [54]. As an essential nutritional component, pantothenol was reported to play an important role in the formation of acetyl-co-enzyme A (acetyl-CoA), which provides activated acetic acid into the citric acid cycle [55]. Acetyl-CoA is essential for diverse metabolic pathways and the biosynthesis of neurotransmitters [56]. Dysregulation of Acetyl-CoA biosynthesis in animal models was found to be associated with abnormal cellular response to oxidative or metabolic stress and neurodegeneration [57]. In our study, decreased hippocampal glutaryl carnitine, l-asparagine and pantothenol was observed in ApoE<sup>-/-</sup> mice as comparing with C57 mice, indicating that the ApoE defect might affect brain function through disturbing the metabolism of pantothenate, acetyl-co-enzyme A and essential amino acids.

After DHA dietary intervention, the significantly differential metabolites including glycerophosphocholine, glycerophosphoethanolamine and glycerophosphoinositol were consistently observed in C57 and ApoE<sup>-/-</sup> mice. As the main initial receptor for DHA, PC leads to the transfer of DHA from PC to PE under prolonged coexistence with fatty acids, suggesting that the presence of DHA can promote the phospholipid remodeling process [58]. These data were in line with our results, demonstrating the DHA-mediated alteration of the glycerophospholipid metabolic pathway. Pooling these findings with the KEGG enrichment analysis results, our data demonstrated a prominent regulating effect of DHA on cerebral glycerophospholipid metabolism. Additionally, we found that, after DHA dietary intervention, ApoE<sup>-/-</sup> mice showed more down regulated metabolites including fatty acyl carnitine, glycerophosphocholine, glycerophosphoethanolamine and triacylglycerol than C57 mice, suggesting a modifying impact of ApoE defect on the response of these metabolites to DHA intervention. The significant metabolic phenotypic differences between C57 and ApoE<sup>-/-</sup> mice following the DHA-fortified diet also involved multiple metabolic pathways such as fatty acids and phospholipids. Consistently, previous studies have showed that DHA supplementation changed the types of phospholipids and fatty acids profile in the brain, demonstrating the modifying impacts of DHA on brain phospholipid and fatty acids metabolism [59].

## 5. Conclusion

In summary, ApoE gene defect can affect brain protein and lipid profiles in mice. LDLR, ABCG1, SORT1, LOX1, Ubl3 and Syt13 are potential molecular targets involved in the DHA-mediated regulating effect in brain of mice. The beneficial effects of DHA may depend on regulating the expression of vesicular transport and neuroprotection-related proteins as well as influencing phospholipid and fatty acids metabolic processes. Our data also indicated the ApoE-dependent regulating effect of DHA intervention on brain lipid and lipid metabolism related molecule expression, and the impacts of DHA on hippocampal lipid metabolism related molecule expression possibly weakened by ApoE defect.

## Funding

This work was supported by the National Natural Science Foundation of China (grant numbers 82173508, 81973027); the Beijing High-level Public Health Technical Personnel Training Program (grant number 2022-3-032).

## CRediT authorship contribution statement

**Xiuwen Ren:** Supervision, Investigation. **Yueyong Wang:** Software, Methodology. **Yu Liu:** Investigation, Formal analysis. **Jiahao Li:** Validation, Supervision. **Ying Wang:** Investigation. **Xiaochen Huang:** Methodology, Investigation, Data curation. **Xixiang Wang:** Software, Methodology. **Xiaojun Ma:** Software, Project administration. **Linzhong Yuan:** Funding acquisition, Conceptualization. **Shaobo Zhou:** Supervision. **Jingjing Xu:** Writing – review & editing, Writing – original draft, Methodology. **Lu Liu:** Writing – original draft, Software.

## Declaration of Competing Interest

The authors declare that they have no known competing financial interests or personal relationships that could have appeared to influence the work reported in this paper.

## Data availability

The data of this study are available from corresponding author for reasonable request. No data was used for the research described in the article.

## References

- [1] M.V.F. Silva, C.M.G. Loures, L.C.V. Alves, L.C. de Souza, K.B.G. Borges, M.D. G. Carvalho, Alzheimer's disease: risk factors and potentially protective measures, *J. Biomed. Sci.* (2019) (2019) 33, <https://doi.org/10.1186/s12929-019-0524-y>.
- [2] J.V.L. Balestrieri, M.B. Nonato, L. Gheler, M.N. Prandini, Structural Volume of Hippocampus and Alzheimer's Disease, *Rev. Assoc. Med. Bras.* (1992) (2020) 512–515, <https://doi.org/10.1590/1806-9282.66.4.512>.
- [3] T.T.T. Tran, S. Corsini, L. Kellingray, C. Hegarty, G. Le Gall, A. Narbad, M. Muller, N. Tejera, P.W. O'Toole, A.M. Minihane, D. Vauzour, APOE genotype influences the gut microbiome structure and function in humans and mice: relevance for Alzheimer's disease pathophysiology, *FASEB. J.* (2019) (2019) 8221–8231, <https://doi.org/10.1096/fj.201900071R>.
- [4] M.F. Lanfranco, C.A. Ng, G.W. Rebeck, ApoE Lipidation as a Therapeutic Target in Alzheimer's Disease, *Int. J. Mol. Sci.* (2020) (2020), <https://doi.org/10.3390/ijms21176336>.
- [5] M.S. Uddin, M.T. Kabir, Mamun A. Al, M.M. Abdel-Daim, G.E. Barreto, G. M. Ashraf, APOE and Alzheimer's disease: evidence mounts that targeting APOE4 may Combat Alzheimer's Pathogenesis, *Mol. Neurobiol.* (2019) (2019) 2450–2465, <https://doi.org/10.1007/s12035-018-1237-z>.
- [6] A.H. Smelt, F. de Beer, Apolipoprotein E and familial dysbetalipoproteinemia: clinical, biochemical, and genetic aspects, *Semin Vasc. Med.* (2004) (2004) 249–257, <https://doi.org/10.1055/s-2004-861492>.
- [7] Y. Zhang, Y. Gu, Y. Chen, Z. Huang, M. Li, W. Jiang, J. Chen, W. Rao, S. Luo, Y. Chen, J. Chen, L. Li, Y. Jia, M. Liu, F. Zhou, Dingxin Recipe IV attenuates atherosclerosis by regulating lipid metabolism through LXR-alpha/SREBP1 pathway and modulating the gut microbiota in ApoE(-/-) mice fed with HFD, *J. Ethnopharmacol.* (2021) (2021) 113436 <https://doi.org/10.1016/j.jep.2020.113436>.
- [8] Y. An, X. Zhang, Y. Wang, Y. Wang, W. Liu, T. Wang, Z. Qin, R. Xiao, Longitudinal and nonlinear relations of dietary and Serum cholesterol in midlife with cognitive decline: results from EMCOA study, *Mol. Neurodegener.* (2019) (2019) 51, <https://doi.org/10.1186/s13024-019-0353-1>.
- [9] L. Dai, L. Zou, L. Meng, G. Qiang, M. Yan, Z. Zhang, Cholesterol metabolism in neurodegenerative diseases: molecular mechanisms and therapeutic targets, *Mol. Neurobiol.* (2021) (2021) 2183–2201, <https://doi.org/10.1007/s12035-020-02232-6>.
- [10] J.E. Vance, Dysregulation of cholesterol balance in the brain: contribution to neurodegenerative diseases, *Dis. Model. Mech.* (2012) (2012) 746–755, <https://doi.org/10.1242/dmm.010124>.
- [11] J. Balakrishnan, S. Kannan, A. Govindasamy, Structured form of DHA prevents neurodegenerative disorders: a better insight into the pathophysiology and the mechanism of DHA transport to the brain, *Nutr. Res.* (2021) (2021) 119–134, <https://doi.org/10.1016/j.nutres.2020.12.003>.
- [12] J. So, B.F. Asztalos, K. Horvath, S. Lamón-Fava, Ethyl EPA and ethyl DHA cause similar and differential changes in plasma lipid concentrations and lipid

- metabolism in subjects with low-grade chronic inflammation, *J. Clin. Lipidol.* 2022 (2022) 887–894, <https://doi.org/10.1016/j.jacl.2022.10.002>.
- [13] C. Cugno, D. Kizhakayil, R. Calzone, S.M. Rahman, G.V. Halade, M.M. Rahman, Omega-3 fatty acid-rich fish oil supplementation prevents rosiglitazone-induced osteopenia in aging C57BL/6 mice and in vitro studies, *Sci. Rep.* 2021 (2021) 10364, <https://doi.org/10.1038/s41598-021-89827-8>.
- [14] S.B. Scheinman, D. Sugasini, M. Zayed, P.C.R. Yalagala, F.M. Marottoli, P. V. Subbaiah, L.M. Tai, LPC-DHA/EPA-Enriched Diets Increase Brain DHA and Modulate Behavior in Mice That Express Human APOE4, *Front. Neurosci.* 2021 (2021) 690410, <https://doi.org/10.3389/fnins.2021.690410>.
- [15] V.A. Duong, H. Lee, Bottom-Up Proteomics: advancements in sample preparation, *Int. J. Mol. Sci.* 2023 (2023), <https://doi.org/10.3390/ijms24065350>.
- [16] J.G. Meyer, N.M. Niemi, D.J. Pagliarini, J.J. Coon, Quantitative shotgun proteome analysis by direct infusion, *Nat. Methods* 2020 (2020) 1222–1228, <https://doi.org/10.1038/s41592-020-00999-z>.
- [17] H. Xiong, D. Callaghan, A. Jones, D.G. Walker, L.F. Lue, T.G. Beach, L.I. Sue, J. Woulfe, H. Xu, D.B. Stanimirovic, W. Zhang, Cholesterol retention in Alzheimer's brain is responsible for high beta- and gamma-secretase activities and Abeta production, *Neurobiol. Dis.* 2008 (2008) 422–437, <https://doi.org/10.1016/j.nbd.2007.10.005>.
- [18] S.S. Meyrelles, V.A. Peotta, T.M. Pereira, E.C. Vasquez, Endothelial dysfunction in the apolipoprotein E-deficient mouse: insights into the influence of diet, gender and aging, *Lipids Health Dis.* 2011 (2011) 211, <https://doi.org/10.1186/1476-511X-10-211>.
- [19] A. Harari, Frenkel A. Leikin, I. Barshack, A. Sagee, H. Cohen, Y. Kamari, D. Harats, Kfir M. Kandel, A. Shaish, Addition of fish oil to atherogenic high fat diet inhibited atherogenesis while olive oil did not, in LDL receptor KO mice, *Nutr. Metab. Cardiovasc. Dis.* 2020 (2020) 709–716, <https://doi.org/10.1016/j.numecd.2019.12.007>.
- [20] F. Matsuura, N. Wang, W. Chen, X.C. Jiang, A.R. Tall, HDL from CETP-deficient subjects shows enhanced ability to promote cholesterol efflux from macrophages in an apoE- and ABCG1-dependent pathway, *J. Clin. Invest.* 2006 (2006) 1435–1442, <https://doi.org/10.1172/JCI27602>.
- [21] Z.W. Zhao, M. Zhang, G. Wang, J. Zou, J.H. Gao, L. Zhou, X.J. Wan, D.W. Zhang, X. H. Yu, C.K. Tang, Astragalus Retards Atherosclerosis by Promoting Cholesterol Efflux and Inhibiting the Inflammatory Response via Upregulating ABCA1 and ABCG1 Expression in Macrophages, *J. Cardiovasc. Pharmacol.* 2021 (2021) 217–227, <https://doi.org/10.1097/FJC.0000000000000944>.
- [22] A. Doublet, V. Robert, B. Védie, D. Rousseau-Ralliard, A. Reboulleau, A. Grynberg, J.L. Paul, N. Fournier, Contrasting effects of arachidonic acid and docosahexaenoic acid membrane incorporation into cardiomyocytes on free cholesterol turnover, *Biochim Biophys. Acta* 2014 (2014) 1413–1421, <https://doi.org/10.1016/j.bbailp.2014.07.003>.
- [23] J. Zou, C. Xu, Z.W. Zhao, S.H. Yin, G. Wang, Asprosin inhibits macrophage lipid accumulation and reduces atherosclerotic burden by up-regulating ABCA1 and ABCG1 expression via the p38/Elk-1 pathway, *J. Transl. Med.* 2022 (2022) 337, <https://doi.org/10.1186/s12967-022-03542-0>.
- [24] A.S. Carlo, C. Gustafsen, G. Mastrobuoni, M.S. Nielsen, T. Burgert, D. Hartl, M. Rohe, A. Nykjaer, J. Herz, J. Heeren, S. Kempa, C.M. Petersen, T.E. Willnow, The pro-neurotrophin receptor sortilin is a major neuronal apolipoprotein E receptor for catabolism of amyloid-beta peptide in the brain, *J. Neurosci.* 2013 (2013) 358–370, <https://doi.org/10.1523/JNEUROSCI.2425-12.2013>.
- [25] K. Saadipour, M. Yang, Y. Lim, K. Georgiou, Y. Sun, D. Keating, J. Liu, Y.R. Wang, W.P. Gai, J.H. Zhong, Y.J. Wang, X.F. Zhou, Amyloid beta(1)–(4)(2) (Aβeta4(2)) up-regulates the expression of sortilin via the p75(NTR)/RhoA signaling pathway, *J. Neurochem* 2013 (2013) 152–162, <https://doi.org/10.1111/jnc.12383>.
- [26] F. Luchetti, R. Crinelli, M.G. Nasoni, S. Benedetti, F. Palma, A. Fraternali, L. Iuliano, LDL receptors, caveolae and cholesterol in endothelial dysfunction: oxLDLs accomplices or victims? *Br. J. Pharmacol.* 2021 (2021) 3104–3114, <https://doi.org/10.1111/bph.15272>.
- [27] L. Yue, J.T. Bian, I. Grizelj, A. Cavka, S.A. Phillips, A. Makino, T. Mazzone, Apolipoprotein E enhances endothelial-NO production by modulating caveolin 1 interaction with endothelial NO synthase, *Hypertension* 2012 (2012) 1040–1046, <https://doi.org/10.1161/HYPERTENSIONAHA.112.196667>.
- [28] Q. Li, Q. Zhang, M. Wang, F. Liu, S. Zhao, J. Ma, N. Luo, N. Li, Y. Li, G. Xu, J. Li, Docosahexaenoic acid affects endothelial nitric oxide synthase in caveolae, *Arch. Biochem. Biophys.* 2007 (2007) 250–259, <https://doi.org/10.1016/j.abb.2007.06.023>.
- [29] J. Laiman, S.S. Lin, Y.W. Liu, Dynamins in human diseases: differential requirement of dynamin activity in distinct tissues, *Curr. Opin. Cell. Biol.* 2023 (2023) 102174, <https://doi.org/10.1016/j.cob.2023.102174>.
- [30] G. Schmitz, M. Grandt, The molecular mechanisms of HDL and associated vesicular trafficking mechanisms to mediate cellular lipid homeostasis, *Arterioscler. Thromb. Vasc. Biol.* 2009 (2009) 1718–1722, <https://doi.org/10.1161/ATVBAHA.108.179507>.
- [31] H. Ageta, N. Ageta-Ishihara, K. Hitachi, O. Karayel, T. Onouchi, H. Yamaguchi, T. Kahyo, K. Hatanaka, K. Ikegami, Y. Yoshioka, K. Nakamura, N. Kosaka, M. Nakatani, A. Uezumi, T. Ide, Y. Tsutsumi, H. Sugimura, M. Kinoshita, T. Ochiya, M. Mann, M. Setou, K. Tsuchida, UBL3 modification influences protein sorting to small extracellular vesicles, *Nat. Commun.* 2018 (2018) 3936, <https://doi.org/10.1038/s41467-018-06197-y>.
- [32] M. Simons, G. Raposo, 2009. Exosomes—vesicular carriers for intercellular communication, *Curr. Opin. Cell. Biol.* (2009) 575–581, <https://doi.org/10.1016/j.cob.2009.03.007>.
- [33] H. Asai, S. Ikezu, S. Tsunoda, M. Medalla, J. Luebke, T. Haydar, B. Wolozin, O. Butovsky, S. Kugler, T. Ikezu, Depletion of microglia and inhibition of exosome synthesis halt tau propagation, *Nat. Neurosci.* 2015 (2015) 1584–1593, <https://doi.org/10.1038/nn.4132>.
- [34] L. Rajendran, M. Honsho, T.R. Zahn, P. Keller, K.D. Geiger, P. Verkade, K. Simons, 2006. Alzheimer's disease beta-amyloid peptides are released in association with exosomes, *Proc. Natl. Acad. Sci. U. S. A.* (2006) 11172–11177, <https://doi.org/10.1073/pnas.0603838103>.
- [35] P.K. Moghadam, M.B. Jackson, The functional significance of synaptotagmin diversity in neuroendocrine secretion, *Front. Endocrinol.* 2013 (2013) 124, <https://doi.org/10.3389/fendo.2013.00124>.
- [36] M. Nizzardo, M. Taiana, F. Rizzo, Benitez J. Aguila, J. Nijssen, I. Allodi, V. Melzi, N. Bresolin, G.P. Comi, E. Hedlund, S. Corti, Synaptotagmin 13 is neuroprotective across motor neuron diseases, *Acta Neuropathol.* 2020 (2020) 837–853, <https://doi.org/10.1007/s00401-020-02133-x>.
- [37] A. Minis, J.A. Rodriguez, A. Levin, K. Liu, E.E. Govek, M.E. Hatten, H. Steller, The proteasome regulator PI31 is required for protein homeostasis, synapse maintenance, and neuronal survival in mice, *Proc. Natl. Acad. Sci. U. S. A.* 2019 (2019) 24639–24650, <https://doi.org/10.1073/pnas.1911921116>.
- [38] M. Hashimoto, [n-3 fatty acids and the maintenance of neuronal functions], *Nihon Yakurigaku Zasshi* 2018 (2018) 27–33, <https://doi.org/10.1254/fpj.151.27>.
- [39] E. Chiefari, D.P. Foti, R. Sgarra, S. Pegoraro, B. Arcidiacono, F.S. Brunetti, M. Greco, G. Manfioletti, A. Brunetti, Transcriptional regulation of glucose metabolism: the emerging role of the hmg1 chromatin factor, *Front. Endocrinol.* 2018 (2018) 357, <https://doi.org/10.3389/fendo.2018.00357>.
- [40] J. Wang, X. Zhao, R. Hong, J. Wang, USP26 deubiquitinates androgen receptor (AR) in the maintenance of sperm maturation and spermatogenesis through the androgen receptor signaling pathway, *Adv. Clin. Exp. Med.* 2020 (2020) 1153–1160, <https://doi.org/10.17219/acem/123355>.
- [41] D. Champagne, J. Rochford, J. Poirier, Effect of apolipoprotein E deficiency on reactive sprouting in the dentate gyrus of the hippocampus following entorhinal cortex lesion: role of the astroglial response, *Exp. Neurol.* 2005 (2005) 31–42, <https://doi.org/10.1016/j.expneurol.2005.01.016>.
- [42] C. Alsayyah, R. Ernst, A lipid hydrolase and a ubiquitin ligase play hide-and-seek in the ER membrane, *Embo. J.* 2022 (2022) e112384, <https://doi.org/10.15252/emboj.2022112384>.
- [43] M. Ruiz, R. Devkota, D. Kaper, H. Ruhanen, K. Busayavalasa, U. Radovic, M. Henricsson, R. Kakela, J. Boren, M. Pilon, AdipoR2 recruits protein interactors to promote fatty acid elongation and membrane fluidity, *J. Biol. Chem.* 2023 (2023) 104799, <https://doi.org/10.1016/j.jbc.2023.104799>.
- [44] A. De Tonnac, E. Labussiere, A. Vincent, J. Mourot, Effect of alpha-linolenic acid and DHA intake on lipogenesis and gene expression involved in fatty acid metabolism in growing-finishing pigs, *Br. J. Nutr.* 2016 (2016) 7–18, <https://doi.org/10.1017/S0007114516001392>.
- [45] S.S. Li, H. Cao, D.Z. Shen, C. Chen, S.L. Xing, F.F. Dou, Q.L. Jia, Effect of Quercetin on Atherosclerosis Based on Expressions of ABCA1, LXR-alpha and PCSK9 in ApoE (-/-) Mice, *Chin. J. Integr. Med.* 2020 (2020) 114–121, <https://doi.org/10.1007/s11655-019-2942-9>.
- [46] M. Vandal, W. Alata, C. Tremblay, C. Rioux-Perreault, N. Salem Jr, F. Calon, M. Plourde, Reduction in DHA transport to the brain of mice expressing human APOE4 compared to APOE2, *J. Neurochem.* 2014 (2014) 516–526, <https://doi.org/10.1111/jnc.12640>.
- [47] A. Martinsen, R.N.M. Saleh, R. Chouinard-Watkins, R. Bazinet, G. Harden, J. Dick, N. Tejera, M.G. Pontifex, D. Vauzour, A.M. Minihane, The Influence of APOE Genotype, DHA, and Flavanol Intervention on Brain DHA and Lipidomics Profile in Aged Transgenic Mice, *Nutrients* 2023 (2023), <https://doi.org/10.3390/nu15092032>.
- [48] G. Petras, M.M. Adam, Phases of the serological response in *Pseudomonas aeruginosa* infections, *Acta Microbiol Hung.* 1987 (1987) 147–157.
- [49] C. Conejero-Goldberg, J.J. Gomar, T. Bobes-Bascaran, T.M. Hyde, J.E. Kleinman, M.M. Herman, S. Chen, P. Davies, T.E. Goldberg, APOE2 enhances neuroprotection against Alzheimer's disease through multiple molecular mechanisms, *Mol. Psychiatry* 2014 (2014) 1243–1250, <https://doi.org/10.1038/mp.2013.194>.
- [50] Y. Hou, X. Lin, Z. Lei, M. Zhao, S. Li, M. Zhang, C. Zhang, J. Yu, T. Meng, Sevoflurane prevents vulnerable plaque disruption in apolipoprotein E-knockout mice by increasing collagen deposition and inhibiting inflammation, *Br. J. Anaesth.* 2020 (2020) 1034–1044, <https://doi.org/10.1016/j.bja.2020.07.054>.
- [51] L.W. Simpson, G.L. Szeto, H. Boukari, T.A. Good, J.B. Leach, Impact of four common hydrogels on amyloid-beta (Aβeta) aggregation and cytotoxicity: implications for 3D models of Alzheimer's Disease, *ACS Omega* 2020 (2020) 20250–20260, <https://doi.org/10.1021/acsomega.0c02046>.
- [52] J. Bouchereau, M. Schiff, Inherited Disorders of Lysine Metabolism: A Review, *J. Nutr.* 2020 (2020) 2556S–2560S, <https://doi.org/10.1093/jn/xxaa112>.
- [53] Y. Numata-Uematsu, O. Sakamoto, Y. Kakisaka, Y. Okubo, Y. Oikawa, N. Arai-Ichinoi, S. Kure, M. Uematsu, Reversible brain atrophy in glutaric aciduria type 1, *Brain. Dev.* 2017 (2017) 532–535, <https://doi.org/10.1016/j.braindev.2017.01.003>.
- [54] Y. Sadakane, N. Fujii, K. Nakagomi, Determination of rate constants for beta-linkage isomerization of three specific aspartyl residues in recombinant human alphaA-crystallin protein by reversed-phase HPLC, *J. Chromatogr. B* 2011 (2011) 3240–3246, <https://doi.org/10.1016/j.jchromb.2011.03.020>.
- [55] D.G. Cotter, B. Ercal, X. Huang, J.M. Leid, D.A. D'Avignon, M.J. Graham, D. J. Dietzen, E.M. Brunt, G.J. Patti, P.A. Crawford, Ketogenesis prevents diet-induced fatty liver injury and hyperglycemia, *J. Clin. Invest.* 2014 (2014) 5175–5190, <https://doi.org/10.1172/JCI76388>.
- [56] T. Lashley, M.A. Tossounian, Heaven N. Costello, S. Wallworth, S. Peak-Chew, A. Bradshaw, J.M. Cooper, R. de Silva, S.K. Srari, O. Malanchuk, V. Filonenko, M. B. Koopman, S.G.D. Rudiger, M. Skehel, I. Gout, Extensive Anti-CoA

- Immunostaining in Alzheimer's Disease and Covalent Modification of Tau by a Key Cellular Metabolite Coenzyme A, *Front. Cell. Neurosci.* 2021 (2021) 739425, <https://doi.org/10.3389/fncel.2021.739425>.
- [57] O. Petrone, S. Serafini, B.Y.K. Yu, V. Filonenko, I. Gout, C. O'Flaherty, Changes of the protein covalent pattern in response to oxidative stress and capacitation in Human Spermatozoa, *Int. J. Mol. Sci.* 2023 (2023), <https://doi.org/10.3390/ijms241512526>.
- [58] P. Monge, A.M. Astudillo, L. Pereira, M.A. Balboa, J. Balsinde, Dynamics of Docosahexaenoic Acid Utilization by Mouse Peritoneal Macrophages, *Biomolecules* 2023 (2023), <https://doi.org/10.3390/biom13111635>.
- [59] G.Y. Sun, M.K. Appenteng, R. Li, T. Woo, B. Yang, C. Qin, M. Pan, M. Cieslik, J. Cui, K.L. Fritsche, Z. Gu, M. Will, D. Beversdorf, A. Adamczyk, X. Han, C.M. Greenleaf, Docosahexaenoic Acid (DHA) supplementation alters phospholipid species and lipid peroxidation products in adult mouse brain, heart, and plasma, *Neuromol. Med.* 2021 (2021) 118–129, <https://doi.org/10.1007/s12017-020-08616-0>.